CRITICAL REVIEWS IN FOOD SCIENCE AND NUTRITION
2026, VOL. 66, NO. 5, 1012–1043
https://doi.org/10.1080/10408398.2025.2538546

Taylor & Francis
Taylor & Francis Group

REVIEW ARTICLE

Toward intelligent 3D food printing: a review on the perspective of materials, fabrication, monitoring, and control

Jaehwi Seol[a,b*], Jinhyun Kim[c*], Yeonggeol Hong[d*], Minseok Cha[e], Sangbae Park[c,f,g], Kyoung-Je Jang[d,h], Soo-Jung Kim[e,i] and Hyoung Il Son[a,b,e]

[a]Department of Convergence Biosystems Engineering, Chonnam National University, Gwangju, Republic of Korea; [b]Interdisciplinary Program in IT-Bio Convergence System, Chonnam National University, Gwangju, Republic of Korea; [c]Department of Biosystems Engineering, Seoul National University, Seoul, Republic of Korea; [d]Department of Bio-Systems Engineering, Institute of Smart Farm, Gyeongsang National University, Jinju, Republic of Korea; [e]Research Center for Biological Cybernetics, Chonnam National University, Gwangju, Republic of Korea; [f]Integrated Major in Global Smart Farm, College of Agriculture and Life Sciences, Seoul National University, Seoul, Republic of Korea; [g]Research Institute for Agriculture and Life Sciences, Seoul National University, Seoul, Republic of Korea; [h]Institute of Agriculture & Life Science, Gyeongsang National University, Jinju, Republic of Korea; [i]Department of Integrative Food, Bioscience, and Biotechnology, Chonnam National University, Gwangju, Republic of Korea

ABSTRACT

Three-dimensional food printing (3DFP) involves the creation of edible products by structuring materials using 3D printing technology. 3DFP has garnered significant attention due to its vast potential in the food industry, offering advantages in food customization, precision, creativity, and reducing waste during food production. The key components of 3DFP include food ink materials, fabrication processes, and sensing and control technologies. This review provides an in-depth examination of these elements. First, it summarizes key considerations regarding material characteristics, and discusses both basic and advanced materials for 3DFP. Next, it explores fabrication processes, including their underlying principles, and highlights advanced 3DFP fabrication methods for producing high-quality printed food products. It also introduces sensing, monitoring, and control strategies to enhance real-time process precision and stability. The review concludes with a discussion on the future directions and prospects of intelligent 3DFP systems.

KEYWORDS

Three-dimensional food printing (3DFP); food ink material; fabrication process; monitoring and control; intelligent 3DFP

1. Introduction

Three-dimensional (3D) printing is an advanced technology that creates 3D structures by layering materials sequentially based on digital designs generated by computer modeling programs (Lv et al. 2023; Wu, Zhu, and Li 2024). Among its various applications, 3D printing in the food industry, known as 3D food printing (3DFP), has garnered significant attention due to its vast development potential. The advantages of 3DFP include customization, precision, creativity, waste reduction, efficiency, and accessibility, making it a promising tool for revolutionizing food production (Wu, Zhu, and Li 2024).

The 3DFP process can be categorized into three phases: the preprinting phase, the printing phase, and the post-printing phase. In the preprinting phase, food inks are prepared, and a 3D digital model is created using design tools such as computer-aided design (CAD) software or a 3D scanner. This model is sliced into layers through a slicing process, generating machine-readable instructions that are then transmitted to the 3D printer for execution (Guo, Zhang, and Bhandari 2019). During the printing phase, food materials are deposited layer by layer to construct the desired 3D structures. This phase allows for precise customization of nutrients, flavors, and ingredients for each layer (Lee et al. 2024). In the post-printing phase, the printed food undergoes additional processes, such as hardening or cooking, to prepare it for consumption (He, Zhang, and Fang 2020).

The quality of 3D-printed food can be improved at each stage of 3DFP. Notably, the printing phase offers significant opportunities for enhancement through the integration of feedback control technology. Figure 1(a) illustrates the feedback control architecture, a system that uses real-time sensing and monitoring to optimize process outputs. Feedback control involves continuously sensing the output of process (i.e., monitoring the system's performance) and making necessary adjustments into the process using a controller based on sensing data, thereby ensuring optimal operation. However, most current 3DFP systems lack feedback control, making it challenging to maintain consistent quality in printed products. To address this limitation, an advanced intelligent 3DFP system

CONTACT Sangbae Park sb92park@snu.ac.kr; Kyoung-Je Jang kj_jang@gnu.ac.kr; Soo-Jung Kim bioksj@jnu.ac.kr; Hyoung Il Son hison@jnu.ac.kr
*These authors contributed equally to this work.

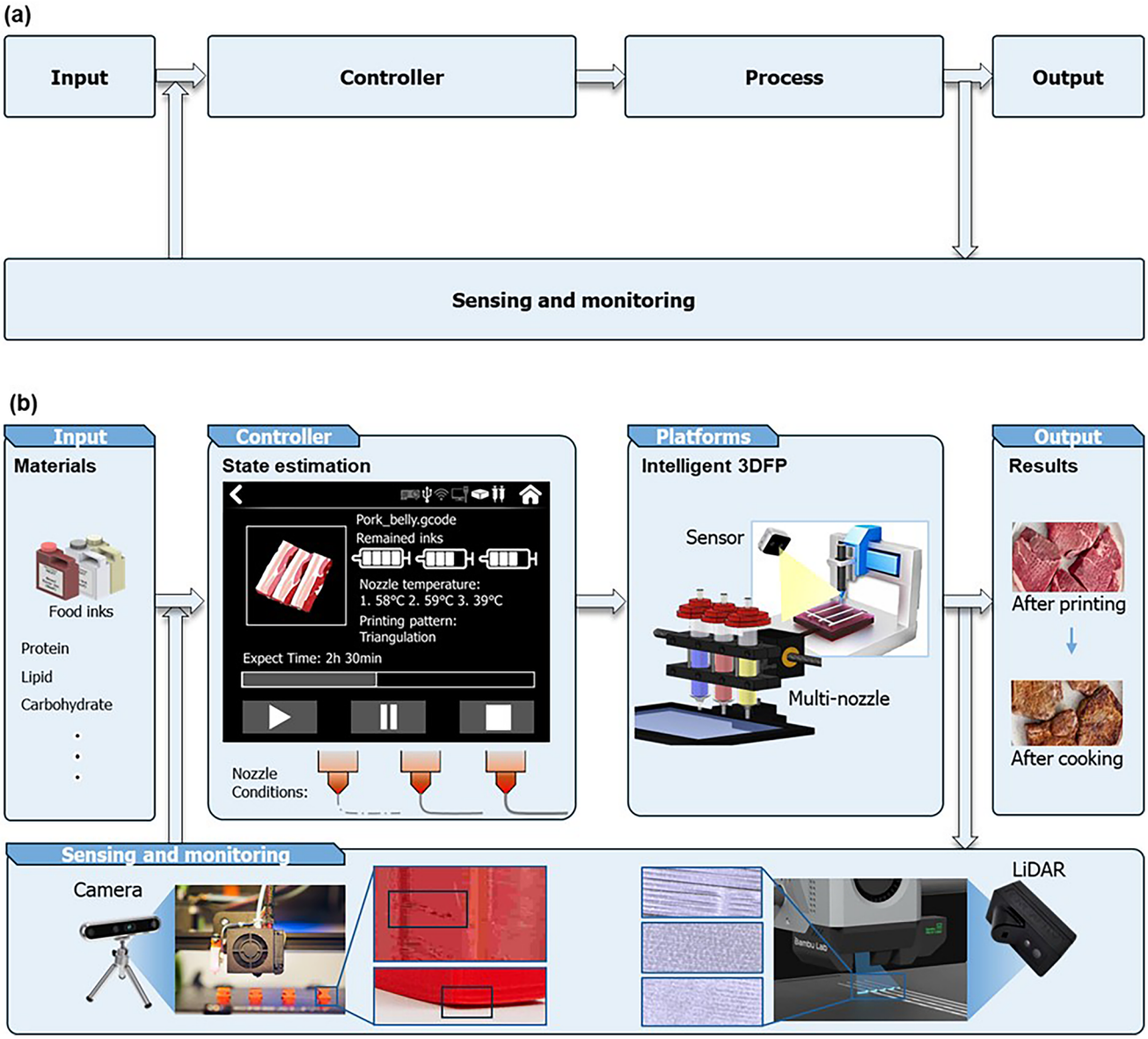

Figure 1. Overview of an intelligent 3DFP system. (a) Closed-loop control structure composed of four main modules: Input, Controller, Process, and Output, with real-time feedback enabled by Sensing and Monitoring. (b) Functional diagram of an intelligent 3DFP system. The Input module provides multi-component food materials such as proteins, lipids, and carbohydrates. The Controller estimates system states and regulates nozzle conditions via pressure, speed, and voltage control. The Process is executed on a multi-nozzle platform equipped with *in situ* sensors. The Output includes results after printing and cooking. Sensing and Monitoring modules, including cameras and LiDAR, collect visual and structural data for feedback to the controller.

is proposed (Figure 1(b)). This system incorporates real-time monitoring and control of parameters such as pressure, printing speed, and voltage to optimize the quality of the final product. By sensing and adjusting in-printing outputs dynamically, the intelligent 3DFP system ensures superior food quality. In the intelligent 3DFP, the control system is closely linked to the fabrication technique, as it must optimize parameter tuning based on the specific printing method. Additionally, the ability to control the fabrication process is directly related to the printability of the food ink. Therefore, comprehensive consideration of material characteristics, fabrication methods, monitoring, and control is essential.

This review explores the key technological elements required to develop intelligent 3DFP systems. The purpose of the intelligent 3DFP system is to improve the existing 3DFP process by integrating cutting-edge technologies such as artificial intelligence, sensors, and automatic monitoring systems to enhance the precision, customization, and efficiency of food production. Furthermore, the system can adapt to various materials, optimize printing parameters in real time, and personalize food according to nutritional needs and preferences. Beyond producing visually appealing food, the system enables customization, personalization, and improved nutritional profiles. This paper is structured as follows: Section 2 explores 3D-printable food materials; Section 3 focuses on fabrication processes, including 3DFP platforms; and Section 4 discusses the sensing, monitoring, and control technologies essential for implementing feedback control architectures. Finally, the review examines the technical limitations of current technologies and discusses future directions for advancing intelligent 3DFP, concluding with key remarks.

2. Materials for 3DFP

In 3D printing, objects are built layer by layer from 2D planes (Shahrubudin, Lee, and Ramlan 2019) using various methods, including extrusion-based 3D printing, photocurable 3D printing, selective laser sintering (SLS), binder jetting, and inkjet printing. 3DFP should have versatility in processing a range of materials (Sun et al. 2018). Also, food inks must meet far more stringent requirements than traditional 3D printing materials, such as filaments and resins since the final product is intended for consumption (Ji et al. 2023). From this perspective, extrusion-based 3D printers are well-suited for processing a variety of food materials while meeting the strict safety and quality standards necessary for consumption. Therefore, in this chapter, we primarily discuss materials suitable for extrusion-based 3DFP. We will comprehensively address food ink systems at the molecular level, specifically how molecular interactions between various components influence the rheological properties and printability. The following subsections review key considerations for selecting food ink materials, then examine a range of basic materials for 3DFP, and finally discuss advanced materials applicable to intelligent 3DFP systems.

2.1. Considerations in materials for 3DFP

2.1.1. Characteristics of ideal food ink

With the growing popularity of 3DFP, a diverse array of food materials has been developed for use as food inks. To ensure suitability, these materials must exhibit the property of printability. Godoi, Prakash, and Bhandari 2016 described printability in terms of a material's behavior during the printing process, including flowability, extrudability, and stability, while highlighted the material's ability to retain dimensional accuracy and conform to predefined shapes post-printing (Godoi, Prakash, and Bhandari 2016; Kadival et al. 2023). In this review, we define printability with a focus on extrudability and self-supporting ability. An ideal food ink with high printability should exhibit sufficient flowability to enable continuous extrusion through the nozzle, while also forming stable structures through its self-supporting behavior during the printing phase.

Ideal food inks should also exhibit key characteristics during both the preprinting and post-printing phases. In the preprinting phase, food inks should be formulated using safe, edible ingredients that offer high nutritional value and are stable for long-term storage. They should also allow for nutritional customization tailored to individual dietary needs. In the post-printing phase, food inks should maintain their structural integrity and preserve their nutritional value during subsequent cooking processes, such as baking, boiling, or deep frying. Food materials that naturally exhibit high printability, or can be engineered to achieve it, should be selected to meet these ideal characteristics. Such materials are essential for producing high-quality, customized, and nutritionally robust 3D-printed foods.

2.1.2. Material-based strategies for achieving high printability: additives

One of the most critical challenges in the 3DFP process arises during the printing phase, where food inks must exhibit conflicting properties before and after extrusion to ensure high printability. Before extrusion, the ink must be sufficiently flowable to pass through the nozzle smoothly, while after extrusion, it must quickly restore adequate mechanical strength to preserve the shape and structural integrity of the printed construct.

To meet these contradictory requirements, two strategies have been proposed (M'Barki, Bocquet, and Stevenson 2017). The first strategy involves using inks with low viscosity and yield stress to facilitate easy extrusion, followed by rapid solidification or gelation after extrusion to achieve high mechanical strength and prevent structural deformation. The second strategy involves using inks with favorable viscoelastic properties, such as shear-thinning and thixotropic behavior, where viscosity decreases under shear stress to enable smooth extrusion, and then rapidly recovers upon stress removal to maintain structural integrity after deposition.

To implement these strategies, additives are commonly incorporated into food materials to enhance their rheological properties and improve printability from a materials perspective. Thermoplastic food materials, such as chocolate, which melts under heat and solidifies at room temperature, are inherently suitable. However, the use of additives broadens the range of applicable materials by enabling the formation of new internal network structures. For example, transglutaminase, which catalyzes the formation of iso-peptide bonds between lysine and glutamine residues, is widely favored as one of the few cross-linking agents that are both edible and effective. By cross-linking protein-based materials that are too liquid to be printable, transglutaminase can convert a liquid-like structure into a gel-like state, enabling smooth extrusion and self-supporting capability after printing (Wang et al. 2023). Optimizing this strategy requires precise control of cross-linking parameters to carefully balance extrudability and self-supporting ability; excessive cross-linking may hinder extrusion, whereas insufficient cross-linking may compromise structural stability post-printing (Song et al. 2021; Tan, Lee, and Hashimoto 2020).

For the second strategy, incorporation of hydrocolloids (e.g., starch, methyl cellulose, xanthan gum, guar gum, alginate, pectin, agar, carrageenan, and gellan gum) can play a key role (Kim, Bae, and Park 2017). While specific molecular mechanisms may vary depending on the type of hydrocolloid, these compounds are generally composed of hydrophilic polymers rich in functional groups that enable extensive water absorption and swelling. Upon hydration, hydrocolloids can form hydrogels, thereby improving ink flowability during extrusion and enhancing shape retention post-deposition by establishing a more stable, self-supporting network (Sharma et al. 2024). In addition, hydrocolloids impart crucial rheological behaviors, such as shear-thinning and thixotropy, that significantly enhance the suitability of food materials for 3DFP (Glicksman 2020).

At the molecular level, shear-thinning occurs as the hydrated polymer chains of hydrocolloids align under shear

stress, reducing intermolecular interactions and thereby lowering viscosity to facilitate smooth extrusion. Once the shear stress is removed, these interactions gradually reestablish, restoring the polymer network structure and viscoelastic properties in a time-dependent manner—a hallmark of thixotropic materials. However, the specific molecular mechanisms of individual hydrocolloids and their interactions with various food materials remain insufficiently understood (Alam et al. 2024). Given that each hydrocolloid exhibits distinct characteristics, such as the ion-induced cross-linking ability of alginate, further investigation into their molecular behaviors and functional roles is essential to advance 3DFP.

Although the two strategies are not clearly distinguishable, the core principle remains the same: transforming otherwise non-printable or only marginally printable food materials into highly printable food inks requires forming or modifying internal network structures through molecular interactions. These networks include not only covalent bonds but also non-covalent intra- and intermolecular interactions. Moreover, additives with heat-resistant properties (e.g., xanthan gum, calcium caseinate, and transglutaminase) have the potential to enhance the structural integrity of printed foods during post-processing steps (Hussain, Malakar, and Arora 2022). Since these processes contribute to improved sensory qualities of the final product (Dankar et al. 2018), additives serve not only as material-based strategies for enhancing printability but also as key contributors to the overall quality of 3D-printed foods. Therefore, future research on additive incorporation in 3DFP should consider their functional roles not only during the printing phase, but also throughout the entire process, including pre- and post-printing phases.

In summary, 3DFP holds significant potential for producing nutritionally customized and structurally complex food products. At the core of 3DFP lies the development of food inks, which requires a comprehensive understanding of food material properties, rheological behavior, and molecular interactions within the food ink matrix to ensure high printability. To address the inherent limitations of 3DFP—particularly the limited range of directly usable food materials—the food industry has incorporated additives such as hydrocolloids. The following subsection reviews the range of food inks developed through ongoing research, categorizing them according to their primary macronutrient composition.

2.2. Basic materials for 3DFP

2.2.1. Carbohydrate-based inks

Carbohydrates are a vital component of the human diet, providing an immediate energy source and replenishing stores between meals. Due to their nutritional importance and widespread use in foods, a variety of carbohydrate-based inks have been developed for 3DFP applications. Among these, starch-based formulations are the most prevalent, owing to their inherent ability to form hydrogels and achieve high printability through gelatinization.

At the molecular level, gelatinization refers to the transition starch undergoes when heated in water, during which the granules swell and lose their semi-crystalline structure, leading to the dispersion of amylose and amylopectin polymers into the surrounding solution (Ratnayake and Jackson 2009). The disruption of preexisting hydrogen bonds and the dispersion of polymers enhance water-engaging capacity by exposing additional hydroxyl groups—a key distinction from gelation, which involves the formation of new polymer networks rather than the breakdown of existing structures. Given these properties, starch has been extensively investigated as a candidate material for 3DFP (Cheng et al. 2023), with numerous studies providing evidence of its suitability for extrusion-based systems. Starches derived from various sources including wheat, rice, potato, and corn have all been shown to be processable into food inks through a simple procedure involving mixing with distilled water and heating. In particular, wheat starch has been shown to yield high-quality and precise prints when prepared using this method (Zheng et al. 2021). Similarly, rice, potato, and corn starches have demonstrated favorable printability, requiring only the heating of their aqueous suspensions to 70–80 °C without the need for additional additives (Chen et al. 2019).

The printability of starch-based inks can be further improved through the incorporation of additives. Additives can influence the internal molecular structure of starch hydrogels either by directly binding and forming complexes with starch (Kadival et al. 2024) or indirectly by limiting the accessibility of water molecules to starch (Xia et al. 2024), thereby enhancing the hydrogel's printability. Additionally, additives can impart functionalities that are not exhibited by pure starch hydrogels (Hassan et al. 2025). Recent research has incorporated not only traditional hydrocolloids but also novel ingredients, and their effects on printability and the underlying molecular mechanisms have been widely explored (Table 1). This includes single macronutrients such as proteins (Kadival et al. 2024) and oils (Bao, Yang, and Jiang 2024), polyphenols (Li et al. 2025; Zeng et al. 2021), hydrocolloids (Liu, Hu, et al. 2025), and natural plant-based components such as leaf powder (Fan et al. 2024) and peel powder (Wedamulla et al. 2024).

These studies focused on incorporating novel ingredients that had not been previously explored. They also provided a precise understanding of how molecular interactions within the ink matrix contribute to enhanced printability, effectively linking molecular-level interactions with macroscopic rheological properties. For instance, Wedamulla et al. 2024 demonstrated that citrus peel powder enhances printability, rheological and textural properties of potato starch hydrogel, and further clarified the mechanisms underlying these effects (Figure 2(a)). They successfully printed a hollow cuboid, achieving a high printing fidelity score. They proposed mechanisms whereby citrus peel reduces the water available for starch granule swelling, thus limiting starch gelatinization and modulating printability to ensure higher-fidelity printed structures. This proposal was further supported by FT-IR data, which confirmed weakened starch-water interactions upon citrus peel addition. Liu, L et al. 2024 developed novel corn starch-based inks incorporating glycyrrhizic acid (GA) and demonstrated that this additive enhanced self-supporting properties and thixotropic recovery. These interactions increased the bound water content in the corn starch-GA

Table 1. Food inks with high printability in three-dimensional food printing (3DFP) and their underlying molecular mechanisms.

Food Ink System			Printability		Underlying Molecular Mechanisms		
Main Material	Additives	Gelation Method	Printed Geometry	Evaluation Metric	Molecular-Level Interactions	Macroscopic Effects on Printability and Structure	References
Carbohydrate-based Inks							
Wheat Starch (WS)	Astragalus polysaccharide	Swell, heat	Cuboid; $21 \times 21 \times 10\,mm^3$	Self-defined metric (CCR); 99.25%	Hydrogen bonds between astragalus polysaccharide and WS; competitive water binding limits starch swelling, enhanced gel network	Improved printing precision and smooth extrusion	(Xia et al. 2024)
	Canola oil	Swell, heat	Cuboid, others; $20 \times 20 \times 10\,mm^3$	Self-defined metric (printing accuracy); 93.3%	Non-covalent (mainly hydrophobic) interactions between canola oil and WS; disrupted amylose-amylopectin interaction	Improved extrusion and shape retention, decreased hardness and chewiness for dysphagia-friendly texture	(Bao, Yang, and Jiang 2024)
	Sodium chloride	Swell, heat	Cuboid; N/A	Max printable height; 42 mm	Na^+ ions interacting with hydroxyl groups in WS; hindered starch polymerization	Improved extrusion, reduced retrogradation, sustained softness and elasticity	(Zheng et al. 2022)
	Whole meal flour	Swell, heat	$ shape; $53.4 \times 32.49 \times 5\,mm^3$	Dimensional accuracy	Proteins, fats, and fibers in whole meal interacting with WS; starch-protein & amylose-lipid complexes confirmed	Reinforced starch gel network, reduced retrogradation, improved water retention, sustained elasticity over time	(Zheng et al. 2021)
Rice Starch (RS)	Algal biomass, millet flour	Swell	Duck, others; $82 \times 36 \times 25\,mm^3$	Qualitative; visual inspection	Bioactive compounds in algal biomass (proteins, polyphenols, polysaccharides) interacting with millet and RS; hydrogen bonding, ester linkages formed	Improved shear-thinning and firmness, enhanced mineral content contributed to nutritional enrichment	(Hassan et al. 2025)
	Peanut protein isolate	Swell, heat	Triangle; N/A	Qualitative; visual inspection	RS and peanut protein; starch-protein complex formation enhanced at low protein concentrations	Increased viscosity and extrusion force at low protein concentration, enhanced structure stability	(Kadival et al. 2024)
	Catechin (CC), procyanidin (PC)	Swell, heat	Double triangle, others; $28 \times 28 \times 25\,mm^3$	Max printable layers: 17 ± 1.41	Polyphenols and starch chains; strong intermolecular interactions disrupted starch gel network	Reduced viscosity, improved extrudability and structural recovery	(Zeng et al. 2021)
	–	Swell, heat	Bowl, others; $28 \times 28 \times 49\,mm^3$	Max printable layers; 60 ± 2.8	Water and RS; gelatinization via granule swelling and hydrogen bonding	Exhibited shear-thinning, thixotropic behavior, and self-supporting property	(Chen et al. 2019)
Potato Starch (PS)	Chlorogenic acid (CA)	Swell, heat	Pentagon; $35 \times 35 \times 8\,mm^3$	Self-defined metric (printing deviation); 0.52% (2D), 5.08% (height)	Chlorogenic acid and sweet potato starch (SPS); weakened double helical structure, inhibited gelatinization, increased free water content and reduced semi-bound water content in SPS gel	Enhanced structural recovery and printing accuracy, reduced hardness and chewiness, improved antioxidant activity suggesting potential for obesity diets	(Li et al. 2025)
	Oyster powder	Swell, heat	Cylinder, others; $\varnothing 28 \times 40\,mm^3$	Qualitative; visual inspection	Protein and PS; heat-induced unfolding of α-helices and β-sheets formation reduced via water competition	Increased storage modulus and rigidity, enhanced printability, and satisfied texture requirements for senior-friendly food	(Han et al. 2025)
	Citrus peel (CP) powder	Swell, heat	Hollow cuboid; $20 \times 20 \times 15\,mm^3$	Self-defined metric (printing fidelity); ≈ 94% (graph-estimated)	CP dietary fibers and PS; reduced starch-water interaction and gelatinization via water competition and hydrogen bonding, forming a denser gel network	High storage modulus and fidelity, enhanced hardness, gumminess, springiness, and chewiness with CP concentration, improved antioxidant activity	(Wedamulla et al. 2024)
	–	Swell, heat	Bowl, others; $28 \times 28 \times 49\,mm^3$	Max printable layers; 17 ± 2.8	Water and PS; gelatinization via granule swelling and hydrogen bonding	Exhibited shear-thinning, thixotropic behavior, and self-supporting property	(Chen et al. 2019)

(*Continued*)

Table 1. Continued.

Food Ink System			Printability		Underlying Molecular Mechanisms		
Main Material	Additives	Gelation Method	Printed Geometry	Evaluation Metric	Molecular-Level Interactions	Macroscopic Effects on Printability and Structure	References
Corn Starch (CS)	Xanthan gum, sodium alginate	Swell, heat	Seal, others; $50\times48.9\times43\,mm^3$	Qualitative; visual inspection	Enhanced hydrogen bonding and electrostatic interactions among xanthan gum, sodium alginate, and CS; promoted compact 3D network formation	Increased viscosity, viscoelasticity, hardness, and thermal stability of CS hydrogel	(Liu, Hu, et al. 2025)
	Glycyrrhizic acid (GA)	Swell, heat	Chinese checker, others; $25\times25\times27\,mm^3$	Self-defined metric (printing accuracy); 96.4%	Hydrogen bonding (CS-CS, CS-GA), hydrogen bonding & π-π stacking (GA-GA); increased bound water content in CS-GA hydrogel	High concentration of GA increased storage modulus, thixotropic recovery, improved self-supporting and printing accuracy	(Liu, Zhao, et al. 2024)
	Momordica charantia leaf powder (MCLP)	Swell, heat	Hollow cylinder, others; $\varnothing20\times20\,mm^3$	Self-defined metric (printing accuracy); ≈ 97% (graph-estimated)	MCLP and CS; physical binding of CS and porous sufaces of MCLP, no chemical bonding observed	Larger MCLP particle size enhanced printing precision and microstructure of gel	(Fan et al. 2024)
	–	Swell, heat	Bowl, others; $28\times28\times49\,mm^3$	Max printable layers; 20 ± 2.8	Water and CS; gelatinization via granule swelling and hydrogen bonding	Exhibited shear-thinning, thixotropic behavior, and self-supporting property	(Chen et al. 2019)
Protein-based Inks							
Gelatin	Cellulose nanocrystals (CNC)	Swell, heat	Cylinder; N/A	Qualitative; visual inspection	Hydrogen bonding between CNC and gelatin; promoted formation of gel network structures	Exhibited favorable rheological properties for 3DFP, oriented alignment of CNCs along printing direction	(Wang, Lu, et al. 2024)
	High acyl gellan gum (HG)	Swell, heat	Hollow cylinder; N/A	Self-defined metrics (deformation, shape inconsistency factor); > 0.56, < 0.016	Hydrogen bonding between water and HG; enhanced water-binding capacity in fish gelatin-HG gels	Exhibited shear-thinning, enhanced mechanical strength and structural stability	(Bian et al. 2024)
	–	Swell, heat	Cuboid, others; $20\times20\times15\,mm^3$	Self-defined metric (printing deviation); ≈ 2.67% (length) ≈ 3.11% (width) ≈ −2.89% (height) (graph-estimated)	Water and salmon skin gelatin (SG); gelation via gelatin swelling and hydrogen bonding	Enabled smooth extrusion through shear-thinning and elastic behavior, formed stable structure after printing	(Carvajal-Mena et al. 2022)
	Transglutaminase (TG)	Swell, heat, enzymatic	2D Grid pattern; $20\times20\,mm^2$	Self-defined metric (printability value); 0.9–1.1	TG formed covalent isopeptide bonds between glutamine and lysine residues of gelatin chains; covalent cross-linked gel network formed	Pre-heating gelatin before TG treatment extended printable time; delayed gelation and reduced viscosity increase	(Tan, Lee, and Hashimoto 2020)
Whey Protein (WPI)	Lotus root whole powder (WL)	Swell, heat	Hexagonal with sqaure hole, others; $20\times20\times26\,mm^3$	Self-defined metric (printing accuracy); > 93%	Hydrogen bonding between starch in WL and WPI, hydrophobic interactions and disulfide bonding among WPI; reinforced protein-starch matrix	Improved printability, enhanced water retention and gel elasticity suitable for dysphagia diets	(Wang et al. 2025)
	Sodium alginate (SA)	Swell, heat	Hollow cylinder; $\varnothing50\times40\,mm^3$	Self-defined metric (comprehensive score); ≈ 93.8%	Hydrogen bonding between SA and WP; heating disrupted internal covalent and hydrogen bonds, promoted free group and hydrophobic interactions	Compacted gel network and increased viscosity, appropriate heating promoted aggregation and structural stability	(Li, Wang, Qin, et al. 2024)
	Micellar casein	Swell, pH, heat	Cuboid; $25\times25\times3\,mm^3$	Qualitative; visual inspection	pH-dependent interactions between κ-casein and denatured WPI; altered micelle surface characteristics	Enhanced aggregation rate at lower pH and higher protein concentrations led to improved printability	(Daffner et al. 2021)

(*Continued*)

Table 1. Continued.

Food Ink System			Printability		Underlying Molecular Mechanisms		
Main Material	Additives	Gelation Method	Printed Geometry	Evaluation Metric	Molecular-Level Interactions	Macroscopic Effects on Printability and Structure	References
Egg White Protein (EWP)	Citric acid (CA)	Swell, heat, pH	Flower, others; N/A	Qualitative; visual inspection	Hydrophobic interactions between CA and EWP; preserved secondary structure with altered tertiary structure due to exposed amino acid residues	Exhibited suitable viscosity, shear-thinning, structural restorability, elasticity, and high printing fidelity	(Zhang et al. 2025)
	Tea polyphenol (TP)	Swell, heat	Circular net, others; N/A	Qualitative; visual inspection	Hydrophobic interactions between TP and EWP; reduced intramolecular hydrogen bonding and β-sheet strength in EWP	Improved structural and thermal stability, reduced water content, denser and homogeneous network	(Liu, Xie, et al. 2024)
	Gelatin, corn starch, sucrose	Swell, heat	Snowflake, others; N/A	Qualitative; visual inspection	Inter-protein interactions; heating reduced intra-protein hydrophobic bonding, facilitating enhanced inter-protein interactions	Improved gel hardness and springiness, enhanced viscosity, extrusion behavior and printability	(Liu et al. 2019)
Soy Protein (SPI)	Chelator-soluble pectin (CSP)	Swell, heat	Hexagon, others; N/A	Qualitative; visual inspection	Hydrophobic interactions and ionic bonding between CSP and SPI; induced stable and robust gel structure	Excellent viscosity, mechanical strength, and rheological properties enabled high-precision printing	(Xie et al. 2025)
	Carrageenan, sodium alginate	Swell, heat	3D mesh; $18.6 \times 18.6 \times 8\,mm^3$	Qualitative; visual inspection	Hydrogen bonding, hydrophobic and electrostatic interactions between polysaccharide and SPI; α-helix into β-sheet transition and dense network formation	Increased viscosity and hardness enabled smooth extrusion, favorable storage modulus and thermal stability supported high-fidelity printing	(Wang, Jiang, et al. 2024)
	White mushroom powder	Swell, heat	Cube, others; $15 \times 15 \times 15\,mm^3$	Qualitative; visual inspection	Hydrogen bonding between bioactive compounds in white mushroom and SPI; reduced water mobility	Enabled smooth extrusion and self-supporting, enhanced visual appeal of dysphagia-friendly foods	(Xiao et al. 2024)
	Cricket fraction	Swell	Parallelogram; $65 \times 25 \times 10\,mm^3$	Qualitative; visual inspection	Water and chitin protein in cricket fraction; enhanced water absorption, contributed to structural strength	Pellet fraction exhibited high recovery rate, enabling stable extrusion and self-supporting printed forms	(Nam et al. 2023)
Pea Protein (PPI)	Strawberry powder	Swell, ultrasonic, microwave, heat	Hollow cylinder; $\varnothing 30 \times 10.3\,mm^3$	Self-defined metric (height, diameter deviation); 0.55%, 0.52%	Type of strawberry powder-PPI interactions not specified; microwave and heat treatments promoted aggregation and network formation	Microwave and heating modifications improved rheology and mechanical strength, enabling self-supporting ability and precision printing	(Xu et al. 2025)
	Cellulose nanocrystals (CNC)	Swell, heat	Cube, others; $10 \times 10 \times 10\,mm^3$	Self-defined metric (height fidelity); 100.7%	Electrostatic repulsion, hydrogen bonding, and van der Waals forces between CNC and PPI; affected secondary structure of PPI, promoted gel formation	Enhanced water-holding capacity and shear-thinning, enabled smooth extrusion and structrual self-support	(Lu et al. 2025)
	Citrus pectin	Swell, ultrasonic, pH	Cone; $\varnothing 20 \times 20\,mm^3$	Self-defined metric (printing deviation); 2.5%	Type of citrus pectin-PPI interactions not specified; ultrasonication influenced protein aggregation	Ultrasonication enhanced hardness, elasticity, improved self-supporting and malleability for 3DFP	(Gu et al. 2024)
	Alginate	Swell, heat	Cylinder; $\varnothing 20 \times 30\,mm^3$	Dimensional accuracy	Interaction between Ca^{2+} released from alginate and PPI; induced coagulation of aggregated protein	Enhanced thermal, rheological, and textural properties, improved extrusion behavior	(Oyinloye and Yoon 2021)
Lipid-based Inks							
Emulsion Gel							
Camellia seed oil	Camellia seed protein (CSP), xanthan gum	Blend, shear, cool	Cylinder, others; $\varnothing 20 \times 10\,mm^3$	Self-defined metric (printing deviation); 0.12%	Hydrogen bonds and electrostatic interactions between xanthan gum and CSP; contributed to high mechanical strength	Exhibited superior rheological performance, improved self-supporting ability	(Lin et al. 2025)

(*Continued*)

Table 1. Continued.

Food Ink System			Printability		Underlying Molecular Mechanisms		
Main Material	Additives	Gelation Method	Printed Geometry	Evaluation Metric	Molecular-Level Interactions	Macroscopic Effects on Printability and Structure	References
Flaxseed oil	Pea protein, inulin	Blend, shear, cool	Heart; N/A	Qualitative; visual inspection	Interaction forces between droplet surface and droplet interstitial particles; strengthened with increasing inulin concentration	Improved viscoelasticity, exhibited high thixotropic recovery and good thermal stability	(Wang, Aluko, et al. 2024)
Soybean oil	Walnut protein, κ-carrageenan (KG)	Blend, shear, high-pressure shear, cool	Moai statues, others; N/A	Qualitative; visual inspection	Hydrogen bonds, hydrophobic interactions, and electrostatic association between KG and walnut protein; increased gel strength	Improved printing accuracy and supporting ability	(Li, Wang, Lv, et al. 2024)
	Soy protein isolate (SPI), transglutaminase	Blend, shear, heat	Apple logo; N/A	Qualitative; visual inspection	Hydrophobic interactions and disulfide bonds dominate emulsion gel structure; DHPM-induced protein denaturation exposed hydrophobic groups, enhancing cross-linking and aggregation	Exhibited remarkable viscoelastic characteristics, shear-thinning behavior, inherent self-supporting properties	(Song et al. 2024)
Corn oil	Sea bass protein (SBP), transglutaminase, astaxanthin	Blend, shear	Apple logo; N/A	Qualitative; visual inspection	Interaction forces between droplet surface and droplet interstitial particles; strengthened with increasing SBP concentration	Exhibited higher viscoelasticity, excellent recovery and thixotropy, with confirmed astaxanthin encapsulation stability	(Zhang et al. 2022)
	Cellulose nanocrystals (CNC), sodium chloride	Blend, shear, high-pressure shear, centrifuge	Cube, others; $10\times10\times10\,mm^3$	Qualitative; visual inspection	Cross-linked CNC network in aqueous phase; surface-adsorbed CNCs shared between adjacent droplets	Exhibited excellent storage stability, shear-thinning behavior, and high solid viscoelasticity	(Ma et al. 2022)
Oleogel							
Soybean oil	Corn starch, xanthan gum	Blend	Letter 'H'; N/A	Qualitative; visual inspection	Capillary bridges formed between hydrophilic starch particles via water; promoted 3D network formation within the oil phase	Demonstrated high print accuracy, shape fidelity, and suitability as edible 3DFP inks, quercetin could be incorporated without significant rheology alteration	(Miao et al. 2024)
Sunflower oil	Lecithin, phytosterol	Blend, heat, cool	Cylinder; $\varnothing10\times25\,mm^3$	Self-defined metric (printability); 96.4%	Needlelike microstructure formed via phytosterol–lecithin co-crystallization; replicated natural fat crystal networks	Exhibited self-supportive structures with high shape fidelity, maintained structural stability for at least 24 h post-printing	(Oliveira et al. 2023)
Medium chain triglyceride (MCT) oil	Ethyl cellulose (EC), PEG40S	Blend, heat, cool	Flower; $38\times35\times4\,mm^3$	Qualitative; visual inspection	Hydrogen bonding between EC and MCT oil; PEG40S aligned along EC backbone and interacted with it to enhance gel hardness and network strength	Enabled smooth extrusion, enhanced shape fidelity, and improved overall printability due to crystalline network formation	(Kavimughil et al. 2022)

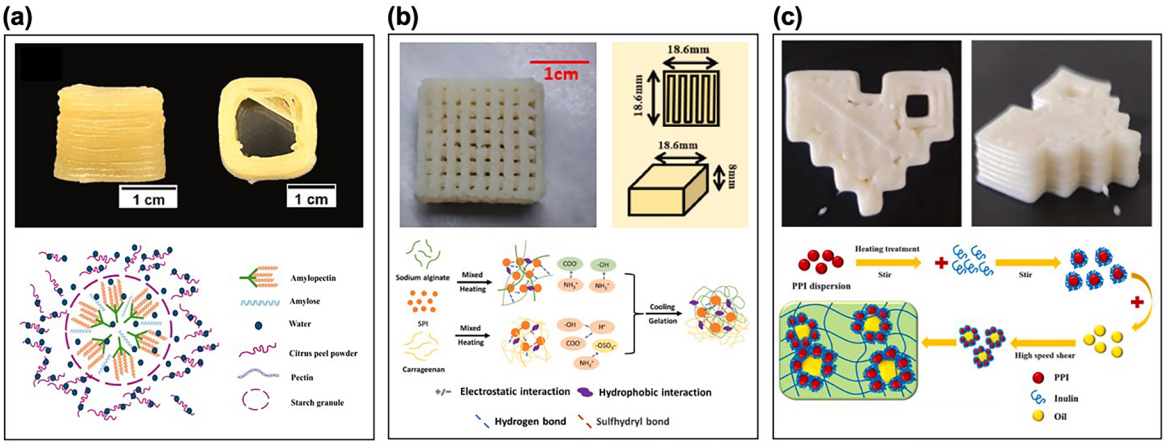

Figure 2. 3D-printed food constructs fabricated using various macronutrient-based inks, along with proposed molecular-level interaction mechanisms visualized in schematic form. (a) Carbohydrate-based inks formulated with potato starch and citrus peel powder. Wedamulla et al. (2024) demonstrated enhanced printability and structural integrity of hollow cuboid constructs ($20\times20\times15\,mm^3$) by incorporating citrus peel powder, which reduced starch gelatinization. The schematic illustrates the interaction between amylopectin, amylose, water, pectin, and citrus peel powder. Reproduced with permission from (Wedamulla et al. 2024) (b) Protein-based inks using soy protein isolate (SPI) in combination with sodium alginate and carrageenan. Wang, Jiang, et al. (2024) identified multiple intermolecular interactions—including hydrogen bonding, hydrophobic forces, and electrostatic interactions—between SPI and polysaccharide additives, which contributed to improved printability of $18.6\times18.6\times8\,mm^3$ mesh constructs. The schematic depicts these interactions between SPI and polysaccharides. Reproduced with permission from (Wang, Jiang, et al. 2024). (c) Lipid-based inks created by emulsifying corn oil with a pea protein–inulin complex. Wang, Aluko, et al. (2024) demonstrated the formation of stable emulsion gels capable of producing high-resolution, heart-shaped structures. The schematic shows the emulsion formation process and the stabilization of oil droplets through interfacial interactions between components. Reproduced with permission from (Wang, Aluko, et al. 2024).

hydrogel, consistent with their FT-IR and NMR data, which confirmed the presence of strong hydrogen bonding. While pioneering studies have begun bridging molecular-level interactions with macroscopic printability, significant knowledge gaps remain. The precise mechanisms between various additives and food materials are still unclear, warranting further investigation.

While starch constitutes the primary component of carbohydrate-based inks, other carbohydrates such as maltodextrin (Montoya et al. 2021), lactose (Fan et al. 2022), and cellulose (Zhang et al. 2024) are frequently incorporated to further tailor the rheological properties of the inks. In particular, cellulose nanocrystals have been reported to enhance shear-thinning behavior, serving as effective rheological modifiers (Armstrong et al. 2022). However, a detailed discussion of these minor carbohydrate-based additives lies beyond the scope of this review, as the primary focus remains on starch-based systems and they will not be further discussed.

2.2.2. Protein-based inks

Proteins are essential macronutrients that play critical roles in growth, tissue repair, and energy supply. In the human diet, proteins provide vital amino acids necessary for maintaining health, and consuming them from diverse sources is recommended to ensure a balanced amino acid profile. Unlike carbohydrates such as starch, single proteins rarely meet the requirements for high printability (Wang, McClements, et al. 2024). To address this, proteins should be combined with additives such as polysaccharides (Li, Wang, Qin, et al. 2024; Wang, Lu, et al. 2024) or other proteins (Liu et al. 2019; Nam et al. 2023). Alternatively, proteins can be modified through physical (Xu et al. 2025), chemical (Daffner et al. 2021), or enzymatic treatments (Tan, Lee, and Hashimoto 2020).

Compared to carbohydrate-based ink, protein-based inks offer considerably greater tunability, not only due to the diversity of their sources but also because of their adaptability in modulating internal network structures via additives, thermal treatment, pH adjustment, enzymatic cross-linking, and other methods. Carbohydrates and proteins share a fundamental characteristic in that both are biopolymers, composed of polymerized sugar monomers and amino acids, respectively. While both consist of linear polymer chains of monomers, proteins typically form more complex structures than polysaccharides (Sui, Zhang, and Jiang 2021). The structure in protein is stabilized through various interactions, including hydrogen bonding, disulfide bridges, hydrophobic interactions, and ionic bonds, both within and between polypeptide chains, resulting in the formation of tertiary and quaternary structures. Since the complex structures of proteins are maintained by weak non-covalent interactions, they are susceptible to denaturation or modification. Consequently, depending on the type and intensity of the applied modification, these structures can be altered in various ways, leading to variability in their resulting functions (Wang, McClements, et al. 2024). Several studies have examined the effects of individual modifications, such as ultrasonication, microwave, and heat treatment, on molecular interactions and printability (Gu et al. 2024; Xu et al. 2025). These modifications solely promoted protein aggregation and network formation favorable for 3DFP.

Through the strategies mentioned above, many food proteins can be processed to form hydrogels suitable for use as food inks in 3DFP (Sharma et al. 2024). Table 1 provides a comprehensive overview of recent studies on protein-based inks with high printability, including their formulations, gelation methods, and underlying molecular mechanisms. Gelatin, derived from collagen, is a fibrous protein widely used as a material for protein-based inks. It forms reversible

cold-set hydrogels below a critical temperature, with water trapped in a network stabilized by hydrogen bonding and hydrophobic interactions. However, due to the weakness of these non-covalent interactions, gelatin cannot retain its shape unless printed in a low-temperature environment (Carvajal-Mena et al. 2022) or stabilized through the formation of permanent isopeptide cross-links catalyzed by transglutaminase (Tan, Lee, and Hashimoto 2020). Gelatin can also interact with hydrocolloids via hydrogen bonding such as with cellulose nanocrystals, which which not only enhances the hydrogel network but also imparts anisotropic alignment (Wang, Lu, et al. 2024).

In contrast, globular proteins such as animal-derived whey protein and egg white protein, as well as plant-derived soy protein and pea protein, form irreversible heat-set hydrogels. When heated above their thermal denaturation temperature, these proteins unfold, exposing non-polar and sulfur-containing amino acids on their surfaces and altering both intra- and intermolecular interaction profiles (Cortez-Trejo et al. 2021). Recent studies have incorporated a diverse array of additives into these globular protein-based systems. Conventional hydrocolloids such as alginate (Oyinloye and Yoon 2021), carrageenan (Wang, Jiang, et al. 2024), and pectin (Xie et al. 2025) have been commonly used, along with proteins like gelatin (Liu et al. 2019). In addition, acids (Zhang et al. 2025), polyphenols (Liu, Xie, et al. 2024), and novel ingredients, including lotus root powder (Wang et al. 2025), white mushroom powder (Xiao et al. 2024), and cricket fractions (Nam et al. 2023), have been explored for their functional and nutritional benefits. Wang et al. identified key intermolecular interactions in soy protein isolate (SPI)-based pastes containing carrageenan and sodium alginate. They showed that carboxyl and hydroxyl groups of the polysaccharides interacted with SPI via hydrogen bonding and hydrophobic forces (Wang, Jiang, et al. 2024). Additionally, the anionic sulfate groups ($-OSO_3^-$) of carrageenan engaged in electrostatic interactions with the cationic groups ($-NH_3^+$) of the protein. These pastes exhibited optimal 3D printing quality when fabricating mesh structures (Figure 2(b)). Despite recent advances, further research is needed to fully understand the interactions between proteins from diverse sources and additives under various modification processes. This knowledge is essential for enabling the fabrication of more complex and innovative protein-based foods, such as plant-based meat analogs (Wen et al. 2023).

2.2.3. Lipid-based inks

Lipids are vital macronutrients essential for growth and proper physiological functioning. In 3DFP, lipids are known for their ability to enhance lubrication, adhesion, mouthfeel, and texture when incorporated as additives in carbohydrate- or protein-based inks (Zhong et al. 2024). Lipid-based inks, in which lipids should serve as the primary component rather than mere additives, commonly utilize emulsion gels and oleogels. These two systems are of particular interest, as they can serve as potential replacements for conventional animal-based fats and as carriers for fat-soluble nutrients (Hu et al. 2023; Pinto et al. 2021). Recent applications of lipid-based ink systems in 3DFP are summarized in Table 1. It includes their additives, which serve as emulsifiers or structuring agents, their gelation methods, printability characteristics, and the molecular interactions involved.

Emulsion gels are semi-solid gel materials with a 3D network structure, in which oil droplets are dispersed throughout a gel matrix (Li, Fan, Liu et al. 2023). Emulsions can be transformed into emulsion gels through two main approaches (Lin, Kelly, and Miao 2020). In the first approach, polymers (e.g., proteins or polysaccharides) in the continuous phase form a supporting gel matrix, within which emulsion droplets are embedded. The structure is referred to as an emulsion droplet-filled gel. In the second approach, emulsion droplets aggregate to form a continuous network themselves, resulting in emulsion droplet-aggregated gels. In this case, the gel matrix is no longer formed by polymers in the continuous phase but arises from the network of interacting emulsion droplets. Although most emulsion gels used in food systems cannot be clearly categorized into one of the two approaches (Wang et al. 2018), their formation generally involves the introduction, alteration or enhancement of interactions either between droplets or between droplets and the gel matrix.

As food-grade emulsions predominantly employ proteins as molecular or particulate emulsifiers (Wang, McClements, et al. 2024), inter-droplet interactions within lipid-based inks can be interpreted in terms of protein–protein interactions. Interactions between droplets and the gel matrix can be interpreted as either protein–protein or protein–polysaccharide interactions. Despite being lipid-based inks, lipids in emulsion gel systems do not directly participate in molecular interactions within the food ink matrix. Rather, they are primarily encapsulated within droplets, making these systems effective for delivering oil and oil-soluble bioactive compounds or nutrients (Yu et al. 2025; Zhang et al. 2022).

Still, lipids must constitute a major portion of the ink. In this regard, oil-in-water (o/w) high internal phase emulsions (HIPEs) and their colloidal-stabilized variants, high internal phase Pickering emulsions (HIPPEs), are promising emulsion gels for lipid-based inks in 3DFP. These systems exhibit viscoelastic, thixotropic, and shear-thinning behaviors, which are critical for achieving high printability in food inks (Gao et al. 2021). Simply increasing the oil fraction can drive gelation through the second approach, as the reduced volume of the continuous phase (water) forces droplets into close contact, forming a continuous network (Lin, Kelly, and Miao 2020). The oil phase in these emulsion gels can consist either of liquid oils or solid fats, such as soybean, almond, peanut, hazelnut, canola, coconut, olive, palm, safflower, sunflower, flaxseed oil, and more (Liu, Cheng, et al. 2025; Li, Fan, Liu et al. 2023).

While lipids themselves do not directly engage in molecular interactions within the matrix, the type of oil used can nevertheless influence the structure of emulsion gels indirectly (Geng et al. 2021). Differences in oil hydrophobicity and interfacial affinity for protein emulsifiers can affect droplet size and distribution, thereby modulating the rheological and mechanical behavior of the resulting emulsion

gel (Chung et al. 2001). Future research should therefore explore the relationship between oil type and emulsion gel performance, with an emphasis on plant-based oils that are low in saturated fats and rich in beneficial unsaturated fats, such as omega-3s.

Adding polysaccharides to the emulsion gel system can further stabilize the network by introducing additional interactions, such as electrostatic interaction, hydrophobic interaction, hydrogen bonding, and disulfide bonding, between proteins and polysaccharides, which help reduce molecular repulsion (Li, Wang, Lv, et al. 2024). Recent studies have incorporated polysaccharides such as xanthan gum, guar gum, locust bean gum (Lin et al. 2025), carrageenan (Li, Wang, Lv, et al. 2024), and inulin (Wang, Aluko, et al. 2024) alongside primary protein emulsifiers, including camellia seed protein, pea protein, and walnut protein. Such incorporations can improve printing accuracy and enhance the shape fidelity of the printed structure. For example, Wang, Aluko, et al. (2024) prepared an emulsion gel by mixing an aqueous pea protein–inulin complex with corn oil, followed by blending (Figure 2(c)). The printability of the gel was further evaluated by printing a heart-shaped structure. None of the printed structures showed signs of collapse, and gels incorporating corn oil with inulin displayed well-defined shapes with precise structural details. The presence of inulin significantly enhanced the ability of pea proteins to stably encapsulate oil. Cross-linking structures were also observed on droplet surfaces, appearing to wrap around them. In addition to protein–polysaccharide complex-stabilized systems, emulsion gels stabilized by protein microgel particles (Song et al. 2024; Zhang et al. 2022) or polysaccharides alone (Ma et al. 2022) are also widely used as lipid-based inks, further expanding the range of emulsion gels applicable to 3DFP.

Oleogels are thermo-reversible, semi-solid lipid mixtures with robust viscoelastic properties (Perța-Crișan et al. 2023; Zhao, Wei, and Xue 2022). They are formed by incorporating oleogelators into liquid oils, which induce the formation of stable 3D networks and transform liquid oils into gel-like materials. Oleogels show great potential in 3DFP due to their unique semi-solid properties, structural stability, and flexibility (Zhong et al. 2024). These systems employ food-grade oleogelators capable of directly structuring edible oils, which can be classified into two categories based on molecular weight: low molecular-mass organic gelators (LMOGs) and polymeric gelators (Co and Marangoni 2018). Substances such as waxes, lecithin, phytosterols, fatty acid derivatives, and monoacylglycerides are examples of LMOGs, while ethyl cellulose is a representative polymeric gelator (Zhao, Wei, and Xue 2022).

For oleogel applications in lipid-based inks, Oliveira et al. developed sunflower oil-based oleogels using phytosterols and lecithin as oleogelators, aiming to harness their synergistic effects (Oliveira et al. 2023). They demonstrated that the resulting oleogel ink exhibited high printability, attributed to the needlelike microstructure formed through the cocrystallization of phytosterols and lecithin. Similarly, Kavimughil et al. (2022) developed medium chain triglyceride-based oleogels incorporating ethyl cellulose with the surfactant polyethylene glycol monostearate (PEG40S) as oleogelators. They found that the addition of the surfactant enhanced printability by optimizing extrusion performance. This improvement was attributed to the formation of additional crystalline structures, as PEG40S interacted along the polymer backbone of ethyl cellulose, reinforcing the overall network. Optimizing the printability of oleogels often requires tuning their crystalline structure, as the self-assembled crystal networks provide the mechanical strength and viscoelasticity needed for extrusion and shape retention. The crystalline structures result forming the molecular crystallization of oleogelators within the oil phase, in contrast to emulsion gels, which depend on dispersed droplets and interfacial interactions rather than crystal formation (Palla, Dominguez, and Carrín 2022; Zampouni et al. 2022).

A recent study further advanced the application of oleogels in 3DFP by fabricating oleogels using hydrophilic corn starch in capillary suspension systems, without the need for chemical modification of the starch (Miao et al. 2024). To address the challenge that starch particles cannot be easily dispersed in oils, a small amount of water was added to a suspension of starch particles in soybean oil. The mixture was then vigorously blended using a stator-rotor disperser. This process induced the formation of a space-spanning starch particle network held together by capillary forces, transitioning the oil system from a fluid-like to a gel-like state. These inks exhibited high printability and demonstrated the ability to incorporate quercetin without significantly altering their viscoelastic properties, highlighting their potential as nutrient delivery systems. Applications of oleogels in 3DFP have only recently been explored and currently occupy a minor position compared to emulsion gels in lipid-based inks. Nevertheless, oleogels are poised to become a key component in the advancement of lipid-based inks for future 3DFP.

2.3. Advanced materials for intelligent 3DFP systems

Intelligent 3DFP not only improve the precision and consistency of printed products but also enable dynamic adjustments during the printing process. To fully leverage the potential of these systems, the integration of basic materials with advanced materials is essential, enabling more efficient, responsive, and synergistic operation. The following subsections introduce two categories of advanced materials: dynamic materials and living materials, which are well-suited for intelligent 3DFP applications and have the potential to drive a transformative shift in the future of food.

2.3.1. Dynamic materials for 4DFP

In four-dimensional (4D) printing, a time axis is added to the conventional three spatial dimensions of 3D printing. As a result, 4D-printed products can undergo predictable changes in response to specific stimuli such as water, heat, magnetic fields, light, or pH. In this context, 4D food printing (4DFP) enables printed foods to respond predictably to environmental stimuli which can trigger transformations in shape, color, taste, texture, and nutritional content (Teng,

Zhang, and Mujumdar 2021). pH-responsive color change is one of the most prominent applications of 4DFP. Su et al. developed nutrient-rich inks composed of purple sweet potatoes, pea protein, and hydroxypropyl methylcellulose, which exhibited visible color changes within the first minute in response to pH variations (Su et al. 2025). Similarly, Zhang & Guo developed dynamic color transitions in multi-material prints by combining purple sweet potato and mashed potato inks, resulting in dynamic color changes as anthocyanins from the inner layer composed of purple sweet potato diffused into the outer mashed potato layers, producing red (acidic), blue-purple (neutral), and green (alkaline) hues (He, Zhang, and Guo 2020). Li et al. formulated an o/w HIPPE-based ink containing curcumin as a pH indicator (Li, Fan, Li, Fan, Li, et al. 2023). Upon heating, the decomposition of sodium bicarbonate produced sodium carbonate, resulting in an elevated pH. This increase in alkalinity triggered a color shift in curcumin from yellow to red, demonstrating thermally induced pH-responsive behavior. Especially, it initiated a multi-step response, wherein heating triggered a pH shift that subsequently caused the color alteration. Also, Phuhongsung et al. demonstrated that 3D-printed foods made from SPI, pumpkin, and beetroot exhibited pH-triggered changes in color, texture, and flavor, allowing for the modulation of attributes such as hardness, gumminess, and aroma (Phuhongsung, Zhang, and Devahastin 2020). With growing consumer interest in interactive and visually engaging foods, 4DFP offers a novel platform for dynamic, customizable color alterations. This not only enhances the esthetic and sensory appeal of printed foods but also enables personalized and immersive dining experiences (Shi, Zhang, and Mujumdar 2024; Wang, Li, Wang, Lv, et al. 2024).

4DFP enables dynamic transformations in shape, nutritional content, and flavor in response to external stimuli. Jiang et al. developed water-in-oil (w/o) HIPPE-based inks incorporating phytosterol nanoparticles and palm kernel stearin, which formed a networked structure that actuated or "bloomed" when exposed to heat (Jiang, Binks, and Meng 2022). This design allowed printed structures to change shape in response to temperature, adding a visually engaging, dynamic element to food products. Similarly, Shi et al. created sunflower oil-based oleogels with beeswax and printed a model that bent under microwave heating (Shi, Zhang, and Phuhongsung 2022). Noree et al. demonstrated shape transformation using inks made from insect powders, achieving thermally driven deformation through dehydration while maintaining protein integrity after heating (Noree et al. 2023). This advancement highlights the potential of protein-based inks to drive sustainable foods with innovative sensory properties. Also, Chen et al. incorporated ergosterol into purple sweet potato-based ink, which converted to vitamin D_2 upon exposure to UV light (Chen, Zhang, and Devahastin 2021). This highlights the potential of carbohydrate-based inks not only to enhance organoleptic properties but also to serve as delivery platforms for nutritional fortification. Phuhongsung, Zhang, and Devahastin (2020) combined SPI with vanilla and κ-carrageenan to enable microwave-induced flavor transformations, resulting in compounds that enhanced bitterness, umami, and saltiness. Together, these advances underscore the multifunctionality of 4DFP materials and their potential to redefine the esthetics, nutrition, and flavor of future food products.

2.3.2. Living materials for bioprinting

Another frontier in intelligent 3DFP systems lies in the using of living materials, or bioinks containing viable cells (Li, Xiang, et al. 2024; Ulagesan et al. 2024). The process of fabricating structures using such cell-laden inks is known as bioprinting, a subfield of 3D printing that aims to replicate biological tissue by spatially organizing cells, biomaterials, and growth factors into functional constructs (Mobaraki et al. 2020). Originally employed in the field of regenerative medicine and tissue engineering, bioprinting is increasingly being explored for food applications (Samandari et al. 2023). In this context, cell-laden bioinks are foundational to the production of cultivated meat and functional cell-based foods, as they are printed into precursor structures of the final products. These constructs are subsequently cultured in bioreactors for a defined period under controlled conditions and further matured by inducing cell differentiation, such as myogenesis of myoblasts in the case of cultivated meat. Through this process, they ultimately develop into fully formed cell-based products. In this food system, the viability and activity of embedded cells contribute not only to the structural fidelity of the printed constructs but also to their nutritional content, flavor profile, and metabolic functionality (Bakhsh et al. 2025; Chandimali et al. 2024).

Notably, food-grade bioprinting was applied to the production of cultured meat using 3DFP (Kang et al. 2021). In this study, a steak-like prototype was engineered by assembling aligned muscle, fat, and blood vessel fibers derived from bovine satellite cells and adipose-derived stem cells. To replicate the hierarchical structure of natural meat, they employed support bath-assisted bioprinting to fabricate fine filamentous fibers from bioinks composed of cells and extracellular matrix components such as fibrinogen and Matrigel. This approach demonstrated not only the structural mimicry of native meat architecture but also the feasibility of producing complex, multicellular edible tissues through bioprinting underscoring its transformative potential within the scope of 3DFP.

This chapter has examined the key considerations and recent progress in materials for 3DFP, with a focus on how molecular-level interactions influence macroscopic printability. Basic materials were categorized into carbohydrate-, protein-, and lipid-based groups, each offering distinct advantages: carbohydrates contribute to structural stability and nutritional versatility, proteins provide tunable rheological behavior and nutritional functionality, and lipids enhance flavor and texture while enabling novel structures through systems like emulsion gels and oleogels. Moreover, we introduced advanced materials supporting intelligent 3DFP systems, including stimuli-responsive dynamic materials that drive 4DFP and living materials such as cell-laden bioinks used in bioprinting of cultivated meat. These innovations enable printed constructs to dynamically change in shape,

color, or nutrition, or to sustain cellular growth and metabolic function. Altogether, this chapter presents a material-centric framework for advancing personalized, responsive, and sustainable food manufacturing. The following chapter transitions to fabrication techniques that bring these inks to function, with emphasis on printing mechanisms, process optimization, and integration with intelligent systems.

3. Fabrication techniques in 3DFP

The performance of 3D printing technology is inherently dependent on the physical and chemical properties of the ink materials used. In the case of 3DFP, an additional constraint is imposed: all components must remain edible even after the printing process. As a result, much stricter limitations apply to material selection and process design compared to conventional industrial 3D printing. It is particularly challenging to achieve food printing quality comparable to that of standard industrial inks such as filaments, resins, or metal powders. To address these limitations, technological approaches have been explored. These include rheological tuning of food materials to improve flowability and viscoelasticity, precise thermal control before extrusion to modify material behavior, and the use of screw-driven extruders to accommodate a wider range of viscosities. Based on these material and process considerations, various fabrication techniques have been developed for 3DFP. Figure 3 provides an overview of these techniques, with schematic illustrations of commonly used methods such as extrusion-based printing, inkjet printing, binder jetting, and selective laser sintering. These methods are categorized from a fabrication technology perspective, with a focus on improving productivity, enhancing print quality, and enabling four-dimensional food printing.

The discussion compares printing methods based on structural characteristics and the relationship between printing techniques and materials. Furthermore, recent studies on 3DFP are examined in the context of the requirements for realizing intelligent 3DFP systems. In addition, the potential impact of applying specialized 3D printing technologies to food printing is analyzed.

3.1. Fundamental technologies of 3DFP

3D printing technologies can be classified according to their operating principles into methods such as Stereolithography (SLA), Digital Light Processing (DLP), Fused Deposition Modeling (FDM), and SLS (Shahrubudin, Lee, and Ramlan 2019). SLA and DLP cure photosensitive resins using ultraviolet (UV) light, FDM extrudes thermoplastic materials by heating and depositing them through a nozzle, and SLS sinters or melts polymer or metal powders using a high-power laser. Although these methods differ in mechanism, they all share the fundamental principle of constructing three-dimensional structures by sequentially stacking two-dimensional cross-sectional layers.

In layer-by-layer 3D printing processes, the material properties must be appropriately controlled to ensure that each deposited layer maintains structural integrity immediately after deposition. In conventional 3D printing, printed materials typically solidify via cooling, curing, or inherent self-supporting characteristics to retain the intended shape. However, in 3DFP, most edible inks undergo minimal

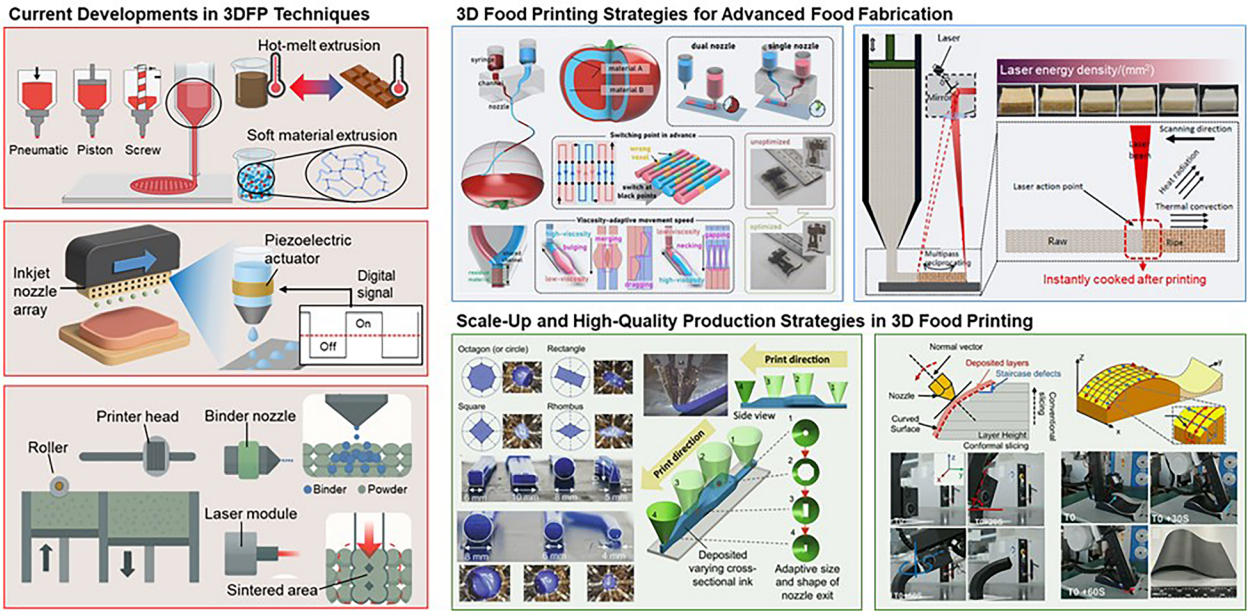

Figure 3. Overview of food fabrication techniques enabled by 3D printing. The section titled Current Developments in 3DFP Techniques presents schematics of three major approaches commonly used in 3D food printing: extrusion-based 3D printing (top), inkjet printing (middle), and powder-based 3D printing (bottom). 3D Food Printing Strategies for Advanced Food Fabrication illustrates techniques such as multi-material 3D printing and post-printing laser-induced modification of ink properties. Reproduced with permission from (Tian, Zhong, et al. 2024) and (Tong et al. 2024). Scale-Up and High-Quality Production Strategies in 3D Food Printing describes the use of adaptive nozzles (AN3DP) and high degree-of-freedom 3D printing systems based on multi-axis robotic arms. Reproduced with permission from (Kang and Mueller, 2024) and (Li et al. 2024).

property changes immediately after extrusion. As a result, the intrinsic rheological properties of the material become the key determinants of printability. Printability can be categorized into two interdependent aspects: (1) extrudability, referring to the material's ability to be efficiently extruded through the nozzle, and (2) self-supporting ability, referring to the ability of the printed structure to maintain its shape without external support. These two characteristics often interact and may even conflict under certain conditions, thus requiring precise tuning between the printing system and material formulation.

Considering such material behavioral characteristics, printability in extrusion-based 3D printing is more appropriately understood not as a single fixed property but as a continuum that reflects the interaction between the material and the printing system. The printing process can generally be divided into two stages: (1) the extrusion of ink through the nozzle under pressure applied by the printer, and (2) the deposition of the extruded material onto the printing bed. In each stage, precise coordination between the rheological properties of the material and the technical specifications of the printing system is required, as this directly influences the fidelity and stability of the printed structure.

3.1.1. Printability based on ink rheological properties; extrudability

In the 3D printing process, various mechanisms, such as pneumatic pressure, syringe pumps, or screw-driven systems, are used to extrude the loaded ink through the nozzle. Complex printing parameters, including the ink extrusion rate and printing resolution, can be influenced by the maximum pressure that the system can supply. The rheological properties of the ink, particularly its viscosity, play a key role in determining the flow rate and must be characterized to appropriately set adjustable parameters such as nozzle diameter, nozzle length, and extrusion speed (Tezel and Kovan 2022). Most inks used in 3D printing exhibit shear-thinning behavior and can be classified as power-law fluids. This behavior is characterized by the flow index n, as described by Equation (1).

$$\eta = K \cdot \dot{\gamma}^{n-1} \tag{1}$$

Where η is the viscosity, K is the consistency index, $\dot{\gamma}$ is the shear rate, and n is the flow index. When $n = 1$, the fluid behaves as a Newtonian fluid with constant viscosity. In contrast, fluids with $n < 1$ exhibit shear-thinning behavior, in which viscosity decreases as shear rate increases. Common examples of shear-thinning food materials include ketchup, jam, and purée. In such cases, viscosity is not only affected by the shear rate but also significantly influenced by temperature; therefore, maintaining a consistent temperature is essential for accurate characterization. Based on experimental conditions such as shear rate and temperature, the flow behavior of the ink can be analyzed to estimate both the consistency index and flow index, ultimately enabling the calculation of viscosity. For shear-thinning fluids, viscosity varies with the applied shear rate. When the volume flow rate is denoted as Q and the nozzle radius as r, the shear rate within a cylindrical conduit such as a nozzle can be defined as shown in Equation (2).

$$\dot{\gamma} = \frac{3n+1}{4n} \cdot \frac{4Q}{\pi r^3} \tag{2}$$

Equation (2), known as the Rabinowitsch-Mooney equation, is a correction formula used to estimate the shear rate of power-law fluids flowing through circular conduits such as pipes or nozzles (Shah 1997). In this context, the volume flow rate is defined by Equation (3).

$$Q = \pi r^2 \cdot V \tag{3}$$

Here, V denotes the velocity of the fluid passing through the nozzle. As shown in Equation (3), the volume flow rate is determined by the nozzle diameter and the discharge velocity of the ink, serving as a key factor in calculating the shear rate for power-law fluids. This illustrates a direct relationship between the printing parameters and the rheological properties of the ink.

Equation (4), known as the Hagen–Poiseuille equation, expresses the relationship between fluid viscosity, flow rate, nozzle radius and length, (L) and pressure.

$$\Delta P = \frac{8\eta QL}{\pi r^4} \tag{4}$$

By analyzing the aforementioned equations, the rheological properties of the ink and relevant printing parameters can be established, enabling the optimization of printing conditions to ensure consistent print quality. Furthermore, calculating the optimal printing speed based on the maximum pressure deliverable by the actuator torque, in accordance with the rheological behavior of food inks, is a crucial factor for achieving scalable commercial food printing. However, accurate estimation of these parameters requires careful consideration of the nozzle geometry, the temperature-dependent flow characteristics of the fluid, and the intrinsic properties of the ink materials. To obtain more precise results, computational fluid dynamics simulations can be employed after modeling the exact geometry in computer-aided design software, allowing for detailed analysis under various physical conditions.

3.1.2. Printability determined by extruded ink geometry; self-supporting ability

Once the material is extruded through the printing nozzle, it is deposited onto the bed or onto the previously printed layer. At this stage, the layer formed by the extruded material must retain its form even after the printing process is complete. The printing conditions related to the material properties of the ink, based on the discussion of printing material conditions by Duty et al. (2018), are summarized in Table 2. Considering that the printed food materials exhibit viscoelastic behavior, this can be briefly explained in terms of the relationship between combined elastic and viscous behavior.

Table 2. Print considerations based on the properties of printing ink.

Case	Fluid behavior	Equation	Features
Elastic-Solid (tan δ < 0.1)	Elastic behavior dominates, and viscous behavior is negligible.	$\epsilon_{limit} > \frac{\sigma_{HP}}{G_0^{'}}$	Printability is evaluated solely based on elastic deformation limits, as viscous behavior is minimal and ignored.
Viscoelastic-Solid (0.1 ≤ tan δ < 1)	Initial elasticity is followed by viscous deformation over time.	$\tau_0 > \frac{-t_{layer}}{ln\left(1-\frac{\epsilon_{limit}\cdot G_0^{'}}{G_0^{'}}\right)}$	Requires consideration of both elastic and viscous deformations during the printing process.
Viscoelastic-Liquid (1 ≤ tan δ < 10)	Continued viscous deformation occurs after initial elastic deformation.	$\eta_0 > \frac{\sigma_{HP}\cdot t_p}{\left(\epsilon_{limit}-\frac{\sigma_{HP}}{G_0^{'}}\right)}$	Elastic deformation limits must be evaluated first, followed by an assessment of cumulative viscous deformation over time.
Viscous-Liquid (tan δ ≥ 10)	Viscous behavior dominates, with negligible elasticity.	$\eta_0 > \frac{\sigma_{HP}\cdot t_p}{(\epsilon_{limit})}$	Printability depends on viscous properties, with the viscosity coefficient determining the deformation rate and stability of the material.

tan δ: Ratio of the loss modulus (G″) to the storage modulus (G′). ϵ_{limit}: Acceptable deformation limit. σ_{HP}: Hydrostatic pressure (entire weight of the deposited ink). $G_0^{'}$: Storage modulus. τ_0: Time constant for deformation response. t_{layer}: Time required for a single layer to settle. t_p: Characteristic processing time. η_0: Viscosity coefficient.

When a sinusoidal strain $\varepsilon(t) = \varepsilon_0 \sin(\omega t)$ is applied, the resulting stress response $\sigma(t)$ for a viscoelastic material is given by:

$$\sigma(t) = \sigma_0 \sin(\omega t + \delta) = \varepsilon_0 G' \sin\omega t + \varepsilon_0 G'' \cos\omega t, \quad (5)$$

where, σ_0 is the amplitude of the stress response, ε_0 is the amplitude of the applied strain, ω is the angular frequency of the oscillation, δ is the phase angle between the applied strain and resulting stress, G' is the storage modulus, representing the elastic (energy-storing) component, and G" is the loss modulus, representing the viscous (energy-dissipating) component. The storage and loss moduli can be derived from the phase angle δ and the ratio of stress to strain amplitude as:

$$G' = (\sigma_0 / \varepsilon_0)\cos\delta, G'' = (\sigma_0 / \varepsilon_0)\sin\delta \quad (6)$$

The loss tangent tan δ, defined as the ratio of the loss modulus to the storage modulus, is a key indicator of the viscoelastic behavior:

$$\tan\delta = \frac{G''}{G'} \quad (7)$$

The storage modulus (G') represents the material's ability to store energy elastically when subjected to an external force, thereby indicating its elasticity. In contrast, the loss modulus (G") reflects the viscous dissipation of energy under deformation, corresponding to the portion of energy lost as heat and not recovered. In purely elastic materials, stress and strain occur in phase, meaning the response of one coincides with the other. In purely viscous materials, strain lags behind stress by a phase angle of 90 degrees. Viscoelastic materials exhibit behavior that lies between these two extremes, with strain showing a partial phase lag relative to stress. From this perspective, the ratio of loss modulus to storage modulus (tan δ) is used as a criterion to classify viscoelastic materials. These characteristics are typically observed through sweep tests using a rheometer. Importantly, viscoelasticity is not a fixed property but varies with changes in amplitude and frequency. Therefore, it is essential to distinguish between the flow behavior of the ink during extrusion through the nozzle and after deposition onto the build plate to fully characterize its rheological properties. In addition to the aforementioned conditions, several other factors must be considered in conjunction, such as the printing conditions for bridges formed when ink is deposited over void spaces in the structure, and the nozzle size, which should be optimized to prevent clogging at the desired print speed.

3.2. Current developments in 3DFP techniques

The manufacturing technology of 3DFP is primarily based on extrusion-based approaches, which have been widely adopted due to their high compatibility with various material properties, the feasibility of multi-material printing, and the simplicity of printer structure. Representative methods include hot-melt extrusion using thermoplastic materials and support bath-based techniques for structural stabilization. These methods follow a common principle of layer-by-layer deposition, where materials are extruded through a nozzle to build structures. In these processes, the extruded ink can maintain its intended shape without excessive spreading (Figure 4(a)). Also, this approach offers high flexibility in structural design. For example, when printing box-shaped structures, the internal volume can either be fully filled or left hollow, and parameters such as infill density can be adjusted accordingly (Figure 4(b)). Moreover, the ability to create a wide variety of internal infill patterns enables the customization of food texture (Figure 4(c)). This level of design freedom is a significant advantage over non-extrusion-based techniques such as SLS or binder jetting, which have limited control over internal fill structures.

However, when printing complex geometries in conventional 3D printing, additional support structures are often required to ensure the structural stability of the printed object. In the case of thermoplastic materials, the printed part and its support are typically made from the same material and designed to allow easy removal after printing. In

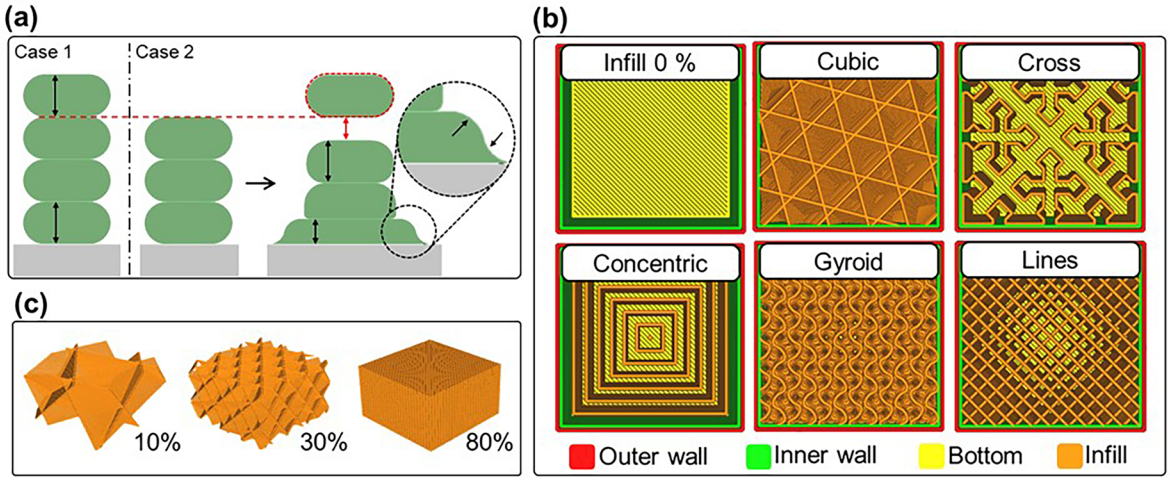

Figure 4. Considerations for various 3D printing techniques. (a) Schematic illustrating self-supporting ability. In Case 1, the structure maintains its shape during layer-by-layer stacking due to sufficient self-supporting ability. In contrast, Case 2 shows deformation of the bottom layer due to insufficient support or the weight of upper layers, resulting in a gap (indicated by the red arrow) between the intended and actual layer height. This gap prevents proper stacking of subsequent layers (dashed red outline). (b) Example settings for various infill patterns and (c) infill density applicable to extrusion-based printing.

contrast, food materials are intended for human consumption and generally exhibit lower durability and shape stability, which makes post-printing support removal more prone to causing deformation or collapse. Due to these limitations, support-less techniques such as SLS and binder jetting have gained attention in 3DFP. These methods offer the potential to fabricate structurally complex food products without the need for additional supports, thereby enhancing the feasibility of high-precision food printing. Meanwhile, there have been efforts to enhance the precision and diversity of printed structures by complementing extrusion-based systems with inkjet printing technologies that operate under different principles. Current strategies in 3D food printing are classified according to printing mechanisms and material properties, as summarized in Table 3.

3.2.1. Extrusion-based 3DFP techniques

Extrusion-based printing generally refers to techniques that deposit high viscosity or semi solid food inks through a nozzle, using mechanisms such as pneumatic pressure, screw-based systems, or piston-driven actuators. In some studies, non-contact printing methods like inkjet printing-based on similar fluid dynamics-have also been utilized to a limited extent. In this section, these techniques are comparatively analyzed based on their extrusion mechanisms and applicable material types.

Food inks used in hot-melt extrusion processes are typically composed of thermoplastic biopolymers such as gelatin and starch, which form solid-like structures through thermal gelation during the cooling stage (Chen et al. 2024; Khan et al. 2022). This gelation is driven by reversible interactions based on non-covalent bonds, such as hydrogen bonding and hydrophobic interactions (Tran, Lee, and Tran 2021). Meanwhile, the incorporation of ionic cross-linking, such as between alginate and calcium ions, reinforces the gel network and enhances structural stability (Sonaye et al. 2022). Although this approach may require additional equipment, such as heating units or cross-linking support systems, it significantly broadens the applicability of food inks by simultaneously meeting the demands for both edibility and mechanical integrity in food printing.

On the other hand, certain food inks are designed to eliminate the need for external equipment by relying solely on their inherent rheological and structural properties. These self-supporting inks can be used to fabricate relatively simple food structures using standard 3D printers. However, since the printability of such materials relies entirely on their inherent physical property, their application scope is inherently limited. To better understand these constraints, it is important to consider the underlying mechanisms that govern phase transitions during printing. At the molecular level, food ink behavior is influenced by transitions such as sol–gel conversion, thermoplastic flow, and ionic cross-linking. These transitions affect structural stability both during and after printing, and are closely linked to the chosen layering strategy and internal architecture.

Unlike typical extrusion-based 3DFP technologies that use pneumatic or screw-driven actuators, inkjet printing employs piezoelectric actuators to eject ink in the form of droplets through ultra-fine nozzles. This method is well suited for the fabrication of highly precise microstructures and is categorized into continuous inkjet and drop-on-demand types, offering resolutions above 70 dpi (Guo et al. 2017). However, inkjet printing is limited to using low viscosity inks (typically below 0.03 Pa·s) which significantly restricts the range of applicable materials compared to extrusion-based methods (Vadodaria and Mills 2020). To construct 3D structures with such low-viscosity materials, post-deposition solidification is essential for maintaining shape fidelity. Yet, many of the curing agents reported to date are not food-safe, prompting ongoing research into curing technologies compatible with edible inks. Oh et al. (2024) demonstrated a cross-linked structure using starch-based ink in a dual-head 3D inkjet printer, where one head dispensed ink containing starch and alginate, and the

Table 3. Current 3D printing techniques.

Printing technique		Material properties	Feature	References
Extrusion-based	Hot-melt	A material with a free phase transition between liquid and solid states depending on temperature.	• By controlling temperature, viscosity and phase transition can be induced, eliminating the need for additional cross-linkers. • To improve print quality, an instantaneous cooling process for high-temperature food ink may be required.	(Liu et al. 2023)
	Soft material (Gelation)	A material capable of gelation through cross-linkers.	• Induces sol-gel transition, transforming solution-based food ink into a gel state immediately after printing. • The edibility of chemical cross-linkers used must be verified. • By adjusting the degree of cross-linking, the mechanical properties of the printed food can be controlled.	(Zhu et al. 2023)
	Self-supporting	A material with sufficiently high viscosity to ensure self-supporting ability.	• Layer-by-layer 3D structures can be printed without additional devices or chemical reactions. • A high-viscosity material extruder is required for printing. • Since printing depends solely on the material properties of the food ink, size, shape, and the number of printable layers may be limited.	(Mu et al. 2023)
Inkjet printing		A material with low viscosity contains sufficiently small particles to pass through an inkjet nozzle.	• Ink sprayed through micro-sized nozzles enables precise and complex structure printing. • The viscosity of the ink used must be low (below 1000 cP). The ink's viscosity, curing properties, and particle content can cause clogging issues in micro-nozzles. • Due to the use of low-viscosity ink, an additional curing process may be required immediately after printing.	(Oh et al. 2024; Zhu et al. 2020)
Binder jetting		A powder-based material combined with an edible binder.	• Forms layers through physical and chemical adhesion between binder and powder. • Can print 3D structures without heating, preventing material deformation and nutrient loss due to heat. • The powder in the printing bath serves as support, allowing complex 3D structures to be printed without additional support structures. • Functional materials can be added to the binder to improve food texture or uniformly incorporate nutrients.	(Chadwick et al. 2024; 2025)
SLS		A material composed of powder with sufficient adhesion strength through laser sintering.	• By adjusting laser power, the texture and mechanical properties of printed food can be controlled. • The powder in the printing bath serves as support, enabling complex 3D structures to be printed without additional support. • Since moisture is not involved in the printing process, this method is suitable for producing snack-type foods. • The shape, size, and uniformity of powder particles directly affect the final print quality.	(Colucci et al. 2024; Jonkers, Dommelen, and Geers 2022)

other sprayed a $CaCl_2$ solution to induce ionic cross-linking. This method achieved over 95% accuracy in both the X and Y directions, and approximately 99% in the Z-axis.

3.2.2. Support-less 3DFP techniques

This section focuses on support-less 3D food printing technologies that can fabricate complex geometries without the need for additional support structures. Representative methods include binder jetting and SLS, both of which utilize the powder bed itself as a supporting medium, thereby simplifying post-processing and enabling high design freedom. In these methods, the shape and physical properties of the printed object are highly sensitive to process variables such as binder dosage, laser energy, and material composition. While the absence of separate support structures simplifies the overall process, the fact that the printed object is completely embedded in the powder bed makes real-time error detection difficult. Therefore, specialized monitoring systems, such as acoustic or thermal sensors, may be required. This section examines the working principles of these two technologies and their applicability to food printing.

Binder jetting is a jet printing method similar to inkjet printing and has been applied to 3D food printing. In this process, a liquid binder is deposited onto a powder bed to bind the particles together and form a 3D structure. Since the powder bed itself serves as the support, complex geometries can be printed without the need for additional supporting structures. This method offers fast printing speeds and is advantageous for achieving intricate food textures. Zhu et al. (2022) used a Z510 3D printer (inkjet printer) to print protein-based snacks, replacing the conventional ink with a 1 mM Tween 20 binder solution and adjusting both

the powder composition and binder dosage. The resulting products had textures similar to crumbled cake or jelly, demonstrating that various textures can be achieved by controlling the combination of binder composition and powder properties.

Sugar or polysaccharide-based binders can enhance binding strength by inducing partial dissolution and recrystallization on the particle surface (Holland, Tuck, and Foster 2018). In addition, incorporating bioactive compounds into the binder allows functional materials to be integrated into the printed structure while retaining their chemical activity without thermal degradation. Since the binder is uniformly distributed across each printed layer, nutrients or functional additives can be evenly incorporated throughout the structure. However, the binder must be food-grade, and its concentration and adhesive strength significantly affect printability and mechanical properties.

Unlike binder jetting, which uses liquid binders, SLS directly sinters powder particles using a laser to form structures. While primarily used for polymer powders, there have also been reports of its application to food materials (Charoo et al. 2020). Jonkers et al. analyzed the microstructure of starch-based prints produced using SLS (Jonkers, Dommelen, and Geers 2022). Their study showed that laser energy density significantly influences the anisotropic stress-strain characteristics of the printed object; at low densities, the horizontal stiffness was approximately three times greater than the vertical stiffness. Furthermore, micro-CT analysis revealed a trend of increased macroscopic damage in the horizontal direction due to interlayer and intralayer defects.

Recent studies have also focused on the physicochemical mechanisms underlying structure formation in SLS-based food printing. In the SLS process, sintering induces interfacial diffusion and physical entanglement through partial melting of particle surfaces. Llamas-Unzueta et al. reported that the SLS process using whey powder involves not only simple thermal fusion but also a complex interplay of various physicochemical mechanisms (Llamas-Unzueta et al. 2025). In whey-based systems, caramelization of lactose and Maillard reactions between proteins occur simultaneously, forming a polymeric cross-linked compound known as melanoidin. As temperature increases, melanoidin's molecular weight also increases, allowing it to function similarly to a thermosetting resin. Melanoidin facilitates interparticle bonding and helps maintain the structure during carbonization. Once the network is formed, it does not remelt, exhibiting irreversible curing behavior. These characteristics explain the improved structural stability of SLS-treated whey powders compared to untreated ones.

3.3. Advanced fabrication technologies for intelligent 3DFP systems

Recently, 3DFP has been evolving beyond simple layer-by-layer deposition. Increasing attention is being paid to the development of intelligent printing systems that integrate artificial intelligence (AI), sensor-based monitoring, and high degree-of-freedom (DOF) printing platforms. These systems can detect printing errors in real time and actively adjust key process parameters. As a result, they help improve structural precision and reproducibility. Advanced printing technologies are now being applied to enable precise deposition of complex multi-material structures and functional food components. These innovations aim to overcome the limitations of conventional 3DFP systems and enhance both print quality and production efficiency.

This section examines the challenges currently faced by 3DFP and reviews recent technological advancements. In particular, it analyzes how these advancements can contribute to the realization of intelligent 3DFP systems through integration with the printing process. The key challenges discussed in this section include: 1), developing advanced strategies for fabricating complex food structures using 3D printing and 2) scaling up production and enhancing the quality of printed foods. Potential strategies for addressing these challenges through 3D printing are explored, along with a discussion on the future potential of these technologies.

3.3.1. 3D food printing strategies for advanced food fabrication

Advanced foods are characterized by structural complexities that are difficult to achieve through conventional cooking methods and can be manufactured using diverse functional food inks. For instance, the nutritional content or physical properties of food can be tailored to meet the dietary needs of patients with dysphagia. Additionally, intricate structural designs may be used to create unique textures that are otherwise unattainable. Furthermore, integrated systems have been developed to enable simultaneous printing and thermal processing, allowing precise control over the degree of cooking throughout the printed structure. While such integrated systems have expanded the capabilities of 3DFP, challenges remain regarding the rheological behavior of food inks and their compatibility with system dynamics. In food printing, the material must retain its shape immediately after deposition, making rheological characteristics a critical factor for print stability. Recently, the demand has expanded beyond mere shape reproduction to include functional structures that respond to environmental conditions. In this context, 4D printing technologies are being introduced into food printing (Navaf et al. 2022). 4D printing involves the design of printed structures that undergo changes in shape or properties in response to external stimuli such as time, temperature, or humidity. Unlike conventional static structures, this dynamic printing technology is now being explored in the food sector, with potential applications in personalized functionality and enhanced consumer interactivity (Navaf et al. 2022).

In 4D printing, the simultaneous deposition of multiple materials is often required, prompting the development of multi-head or multi-nozzle printer systems. These systems help reduce printing errors during material switching by maintaining extrusion continuity, even when syringes are replaced (Lee et al. 2024). However, as the number of printing materials increases, so does the number of required

nozzles, significantly increasing the complexity of the hardware and process control. To alleviate this complexity, single-nozzle-based 3D printers have been developed (Lee et al. 2024). These devices adopt a microfluidic-inspired design, in which multiple material input channels converge into a single output path. Compared to multi-nozzle systems, this configuration has demonstrated reduced material switching times and approximately 38% shorter total printing times relative to syringe-based systems (Tian, Wu, et al. 2024). Nevertheless, one limitation is that residual ink remaining in the conduit after the branching point may interfere with the flow of subsequently deposited materials.

In single-nozzle-based printing systems, differences in rheological properties between various materials can lead to fluctuations in extrusion pressure, resulting in imbalances in extrusion speed. To address this issue, Tian et al. developed a single-nozzle food printing system equipped with an algorithm capable of real-time control of extrusion flow rate and nozzle speed (Tian, Zhong, et al. 2024). This system successfully demonstrated continuous transitions between materials of different viscosities by precisely printing 3D structures composed of mashed potatoes (viscosity: 3.17 Pa·s at a shear rate of 102 s^{-1}) and modified ketchup (viscosity: 1.41 Pa·s), confirming its feasibility for multi-material deposition.

In single-nozzle multi-ink 3D printing systems, print quality is significantly influenced by differences in yield stress between inks during material switching. When inks with different viscosities and rheological properties are used consecutively, backflow or mixing can occur during the transition, compromising the precision and stability of the printed structures. To address this issue, Lee et al. introduced a design strategy that adjusts the offset distance from the ink switching point to the nozzle outlet, as well as the nozzle diameter (Lee et al. 2024). This approach enabled stable, continuous printing even with ink pairs exhibiting yield stress differences greater than 100-fold. Furthermore, the single-nozzle system demonstrated approximately 38% shorter overall printing time compared to multi-syringe systems, highlighting its potential for improving the efficiency of multi-ink food printing. Building on this, Tian et al. quantified the residual ink volume within the transition region and developed a correction algorithm that compensates for offset distance (Tian, Zhong, et al. 2024). The algorithm calculates optimal correction values based on process parameters such as nozzle speed, nozzle length, and ink flow rate. Application of this method reduced printing errors during ink switching by 74%.

In addition to challenges related to ink switching and rheological control, post-processing considerations such as thermal treatment are also critical for ensuring the final quality of printed food products. Because materials suitable for 3D food printing are often paste-like or puréed in nature, printed foods may require further cooking to become ready for consumption. This is especially true for high-protein foods such as meat or fish, where precise shaping via printing necessitates a subsequent thermal treatment. In this context, Blutinger et al. developed a precision cooking system utilizing multi-wavelength lasers (Blutinger et al. 2021). The system combines blue, near infrared, and mid-infrared lasers to heat, sear, and cut the printed food products. In an experiment involving chicken cooked with an IR laser, the surface browning effect was successfully induced, while the cooking loss was reduced by approximately 50% compared to conventional oven cooking. Laser-based technologies enable the integration of 3D printing and cooking without the need for separate post-processing, achieving both surface browning and internal thermal processing simultaneously. As a result, they effectively enhance both the texture and visual appeal of the final product. This approach is gaining attention as a promising method to significantly improve the practicality and manufacturing efficiency of 3D food printing through a streamlined print-to-cook workflow.

Tong et al. incorporated laser sintering technology into an extrusion-based food printing process (Tong et al. 2024). In their study, the surface of surimi ink was sintered using a laser to simultaneously improve both gel strength and printing accuracy. The localized thermal energy from the laser precisely induced the thermal gelation of fish proteins, thereby enhancing the mechanical strength of the printed structure and helping to maintain the intended shape. Notably, the gelled surimi acquired self-supporting ability, enabling structural stability without the need for additional curing agents. Furthermore, by adjusting the laser output conditions, the physical and sensory properties of the final product could be finely tuned. This technology is thus considered highly promising for the production of functional, customized foods in the context of future intelligent 3DFP systems.

3.3.2. Scale-Up and high-quality production strategies in 3D food printing

In 3D printing, there exists a fundamental tradeoff between printing resolution and printing speed. Increasing the nozzle size results in faster deposition and higher throughput but compromises resolution due to the larger ink volume dispensed. Most conventional 3D printers operate with a single printing head on a Cartesian coordinate system. When multiple printing heads are employed simultaneously, mechanical interference between heads can occur, especially in complex geometries. This section reviews recent studies addressing these limitations and discusses how each approach contributes to the scalability and quality control of 3DFP.

In extrusion-based 3D printing, nozzle diameter serves as a critical process parameter and is typically fixed during printing. However, Kang et al. recently proposed an adaptive nozzle (AN3DP) technology that enables real-time adjustment of nozzle diameter and cross-sectional shape during the printing process (Kang and Mueller 2024). The system comprises a pin array of eight individually controllable pins and a flexible membrane. Each pin is connected to a stepper motor and can retract inward or extend outward, deforming the membrane and thereby modifying the nozzle's diameter and shape. The system allows diameter modulation within a range of 3 mm to 10 mm, and the cross-sectional profile can be dynamically altered into various shapes such as circular, square, or star patterns. This approach minimizes printing paths and reduces total printing time. Furthermore,

by integrating with slicing software, it enables optimization of nozzle geometry and toolpaths. As such, AN3DP holds promise as a technology that can enhance both high-resolution output and production efficiency, thereby increasing the potential for large-scale manufacturing and commercial expansion of 3DFP.

Most 3D printers employ a Cartesian coordinate system based on movement along the X-Y-Z axes, which imposes constraints on the printing path. Conventional 3D printing relies on planar stacking along the Z-axis, which inherently leads to a staircase effect when fabricating curved structures. Unlike traditional X-Y-Z axis-based vertical layer-by-layer printing systems, multi-axis printing allows nozzle trajectories to be spatially designed in 3D, thereby achieving higher geometric fidelity. Multi-axis systems enable non-planar nozzle paths that allow continuous formation of curved surfaces within a single layer. As a result, vertical resolution and surface curvature accuracy are significantly improved.

Li, Liu, et al. (2024) demonstrated a system in which a screw extruder was mounted on a 6-DOF robotic arm, successfully printing complex geometries such as curved shells and twisted hollow tubes without the need for support structures. While a conventional Cartesian-based system required 122.3 g of material to fabricate the structure along with its support, the multi-axis system achieved the same geometry using only 62.23 g. By eliminating the need for support structures, material consumption was significantly reduced and the risk of damage during post-processing was minimized. This is particularly advantageous for soft or highly viscous food materials, which are prone to structural deformation when support structures are removed. Multi-axis printing technology, capable of stable layer-by-layer deposition without support structure, is thus considered highly suitable for food printing. With its superior performance in terms of precision, material efficiency, and print stability, multi-axis printing can serve as a foundational technology for next generation 3DFP processes.

The flexible design of nozzle trajectories in multi-axis systems can also be effectively leveraged for the integrated printing of functional materials and structural components. Bao et al. developed a hybrid system equipped with two robotic arms, each fitted with a different printing module: fused filament fabrication using PLA filament for structural construction, and direct ink writing using silver paste for functional material deposition (Bao et al. 2023). This system successfully fabricated highly functional 3D electronic components such as double-helix sensors and multilayer circuit boards by integrating structure and function in a single process. Such a platform holds great promise for intelligent 3DFP applications, including functional food constructs and customized nutrient delivery systems. Moreover, multi-axis printing systems offer high potential for production efficiency through simultaneous multi-material deposition and parallel processing using multiple robotic arms. Each arm operates independently and can follow collision-free nozzle paths, allowing for rapid fabrication of complex structures. This capability presents a significant advantage in the mass production of high-value-added food products.

In addition, printing systems capable of non-planar path setting can directly print on irregular surfaces, enabling applications that add special structures or textures onto existing food substrates. To realize this, tight integration is required among sensor systems that can accurately recognize the shape of the build plate, slicing software that can optimize the printing path, and control algorithms. If a system can recognize the printing environment in real time and dynamically adjust the toolpath, multi-axis printing technology can serve as a key foundational platform for implementing intelligent 3DFP systems. These developments not only enable high-resolution structural printing, but also lay the foundation for multi-functional food constructs, complex geometries, and scalable production with high reproducibility, thereby accelerating the transition toward personalized food design.

4. Sensing, monitoring, and control in 3DFP

To fully realize aforementioned tailored and structurally complex food products, real-time sensing and control mechanisms must be incorporated into the fabrication process. The intelligent 3DFP system, illustrated in Figure 1(b) represent as an advanced approach to 3DFP. It enables real-time control of parameters of 3DFP such as pressure, printing speed, and voltage by continuously sensing and monitoring the quality food during the printing process, ultimately enhancing the quality of the final product. One of the key challenges in 3D printing is the occurrence of errors and defects in the printed objects, as summarized in Table 4. These errors often arise during fabrication, and most 3D printers continue printing despite defects in the output. To address this, recent research has prioritized real-time error correction to improve the quality of printed objects, rather than simply completing the input model irrespective of defects.

Research in 3DFP has focused on the critical roles of sensing, monitoring, and control systems to enhance the quality of 3D-printed food. Sensing technologies detect and assess material properties and conditions with precision, while monitoring systems oversee the process and output quality in real time, identifying deviations from the desired outcomes. Control systems utilize this feedback to adjust parameters dynamically, maintaining optimal printing conditions and ensuring high-quality outputs. The integration of sensing, monitoring, and control technologies is pivotal in optimizing the overall printing process. This integrated approach significantly enhances the efficiency, safety, and quality of 3D-printed food, representing cutting-edge advancements in the final stages of 3D printing, as illustrated in Figure 1(b).

Advancements in the industrial sector have emphasized enhancing the accuracy of 3D printing through machine vision and AI for real-time output monitoring and control. These technologies improve the quality and reliability of 3D printing processes by automating error detection and correction. However, the development of such technologies in 3DFP lags behind conventional 3D printing. Bridging this gap requires further research and innovation to achieve

Table 4. 3D Printing errors during the printing phase.

Printing phase	Specific errors		Reference
Preprinting phase	File format conversion error		
	Slicing error		(Tamir et al. 2022)
	Design error		(Charalampous et al. 2021)
Printing phase	Processing parameter setting error	- Print speed - Temperature setting - Extruder clogging	(Cai et al. 2024)
	Machine error	- Machine vibration - Material deposition process - Calibration of the 3D printer mechanism	(Qian et al. 2024)
Post-printing phase	Errors caused by deformation during removal of support structures		(El Moumen, Tarfaoui, and Lafdi 2019)
	Post-curing and surface treatment errors		(Impens and Urbanic 2016)
	Residual stress		(Alzyod and Ficzere 2023)
	Infill density errors		(Aydin et al. 2022)
External disturbances	Material bending caused by the cooling system		
	Material properties	Material humidity	

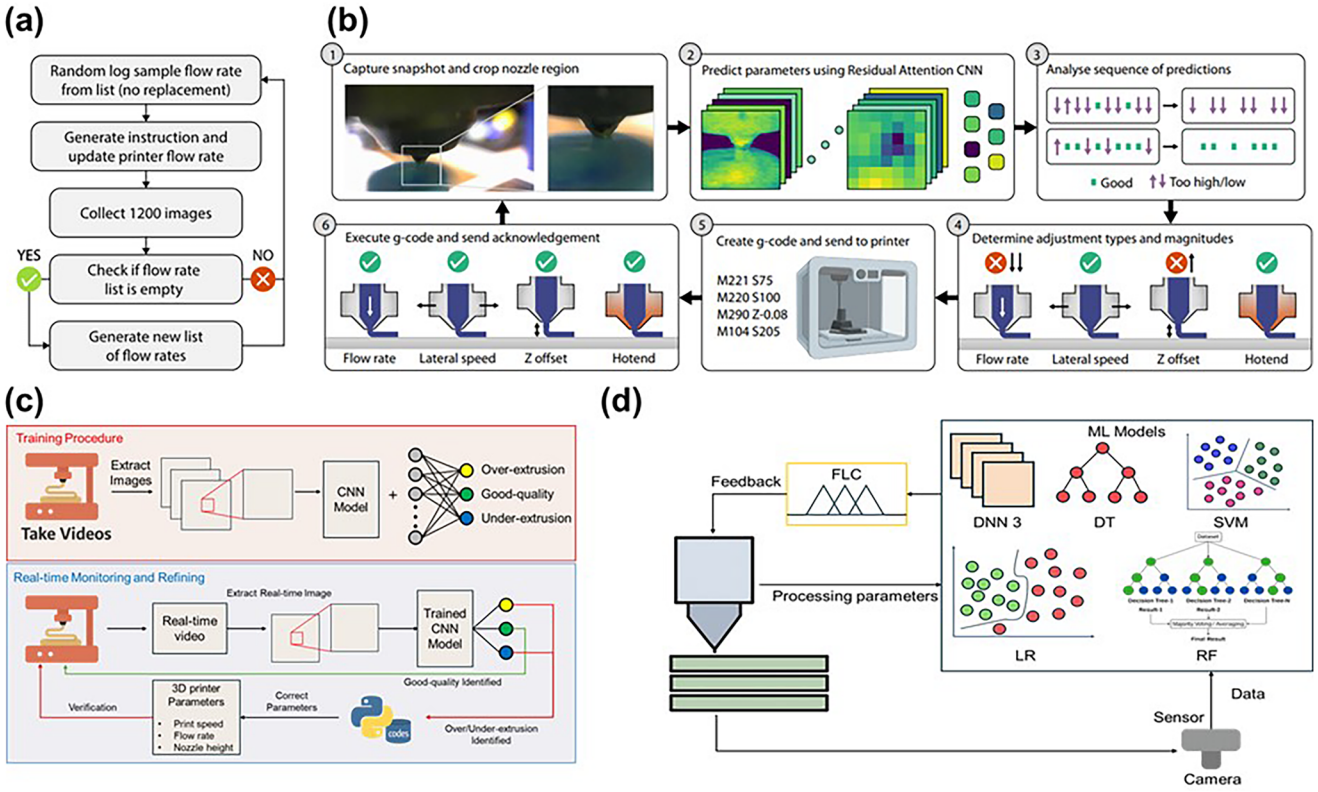

Figure 5. Sensing, monitoring, and control systems: (a) Fast control loop for 3D printing parameter discovery and few-shot correction (Brion and Pattinson 2022a). (b) A machine vision-based control pipeline that captures nozzle images, predicts process parameters using a CNN with residual attention, analyzes sequential outputs, determines correction types and magnitudes, and updates g-code instructions for closed-loop control (Brion and Pattinson 2022b). (c) A real-time monitoring and refinement framework that combines offline training with online inference, where a trained CNN model classifies extrusion quality and guides parameter adjustments during printing. (d) A feedback architecture that integrates sensor and camera data with fuzzy logic controllers and various machine learning models (DNN, RF, SVM, DT) to optimize processing parameters in real time.

comparable precision and reliability. This section reviews existing sensing, monitoring, and control methods in 3D printing and explores ongoing research efforts to advance these technologies in 3DFP. Figure 5 provides an overview of sensing, monitoring, and control systems.

4.1. Sensing in 3DFP

Sensing in 3DFP refers to the detection and evaluation of material properties and environmental conditions both prior to and during the printing process. It plays a critical role in optimizing printer performance and ensuring the quality of the final product. By providing accurate information about system conditions, effective sensing minimizes fabrication errors and enhances reliability throughout the printing workflow. Current sensing technologies typically monitor parameters such as nozzle and bed temperatures; however, although real-time monitoring of printed structures is technically feasible, the resulting data is rarely employed for immediate process control. A major limitation is the occurrence of layer misalignment caused by discrepancies between the

actual printed geometry and the nominal design (Delli and Chang 2018). Furthermore, users often lack real-time reference data to evaluate print accuracy, as feedback regarding the evolving shape of the component during layer-by-layer deposition is generally unavailable.

Efforts to address these issues include advancements in real-time evaluation methods during sensing. Machine vision applied to detect surface defects such as pits, bubbles, and bulges, classifying these as errors in the printed output (Zhou et al. 2024). A key contribution of this research is the adoption of an inclined camera configuration to address the limited field of view inherent in conventional vertically mounted setups, thereby enabling more effective real-time monitoring. However, they mentioned that their research is not yet appropriate for industrial or commercial implementation due to the experimental constraints of 3D printing and the requirement for post-processing. In other research, a multi-camera system consisting of six high-resolution cameras has been employed to enhance visual sensing in 3DFP (Singh et al. 2025). By capturing the printing process from multiple angles, the system enables reliable detection of various defects, including warping and layer delamination. This multi-view configuration significantly improves coverage and detection accuracy compared to single-camera setups.

Similarly, other studies introduced a method to assess printing accuracy using layer-wise image analysis (Ma et al. 2023). By comparing the printed object to the original digital design, this method quantifies inaccuracies such as over-extrusion and under-extrusion, leading to enhanced precision in the printing process. Comparison with human evaluations revealed that the digital tool was more sensitive in detecting subtle defects, particularly under-extrusion, suggesting its usefulness in improving the reliability of quality assessment. However, such machine vision systems are highly sensitive to variations in lighting conditions, often resulting in inconsistent outputs depending on the timing and angle of illumination. To address this limitation, recent approaches have focused on controlling lighting environments or leveraging deep learning-based artificial intelligence techniques that can adapt to diverse illumination scenarios, thereby improving the robustness and reliability of visual analysis.

The aforementioned AI-based solutions were first applied in the field of general 3D printing. For example, regression-based machine learning algorithms have been developed to predict dimensional deviations between CAD models and printed parts. (Charalampous et al. 2021). Similarly, a convolutional neural network was developed for real-time defect detection, reducing production losses and human intervention by identifying geometric anomalies such as inconsistent extrusion, weak infill, lack of support, and sagging (Khan et al. 2021). This study assumes that defects in 3D printing result in geometric distortions within the infill pattern and that these distortions can be detected from a top-view perspective. However, such assumptions lead to limitations; for example, as noted in Zhou et al. (2024) defects may not be visible from the vertical plane. Moreover, the authors acknowledged the limited size of the training dataset, which may reduce the reliability of the proposed method.

Previous studies primarily focused on applying deep learning techniques to implement defect detection in 3D printing. In contrast, defect detection was further improved through the introduction of an enhanced YOLOv8 model, which included an additional feature extraction layer integrated into the original YOLOv8 architecture (Karna et al. 2023). This advancement highlights the potential of AI in smart manufacturing. In the context of 3DFP, understanding and analyzing material properties is particularly important, as they directly impact print quality. Adjusting printing parameters based on the specific characteristics of each material enables process optimization, resulting in more precise and reliable outcomes.

4.2. Monitoring in 3DFP

In 3DFP, monitoring refers to the real-time supervision of the printing process to ensure that each stage is executed as intended and that the final product meets predefined quality standards. Unlike sensing, which evaluates material properties before printing, monitoring focuses on in-process assessment by identifying and correcting errors as they occur during fabrication. Monitoring in 3DFP plays a crucial role in ensuring process consistency and product quality; however, several technical challenges persist in its implementation. The use of multiple sensors, such as vision systems, thermal cameras, and environmental sensors, results in the generation of large volumes of heterogeneous data. Processing this data in real time for accurate detection of deviations requires efficient algorithms and robust data handling frameworks. In particular, distinguishing between acceptable process variability and true anomalies remains a non-trivial task, especially when dealing with soft and deformable food materials.

To ensure structural accuracy and geometric consistency, monitoring systems track key parameters such as layer deposition, extrusion rate, and printing speed. These systems facilitate the detection of common defects, including misalignment, irregular layer thickness, and incomplete deposition. A vision-based method was proposed that performs real-time scanning, filtering, segmentation, and registration of the printed structure against its corresponding digital 3D model. This approach leverages high-resolution point cloud data to enable continuous performance evaluation and early defect detection throughout the printing process (Charalampous et al. 2021). This approach facilitates early-stage defect detection, enabling comprehensive quality assessment without interrupting the printing process. Optical monitoring methods have also been introduced to track the structural evolution of printed layers, particularly in repeated or drift-prone geometries. A cell-based segmentation algorithm was proposed to fragment each layer's nominal image into structural cells for localized defect identification (Gugliandolo et al. 2022).

In addition to ensuring geometric consistency, monitoring of temperature and humidity is critical for maintaining the textural integrity and structural stability of food products. Monitoring systems continuously measure the temperature of both the ambient environment and the extruded food

materials to ensure thermal conditions remain within optimal bounds. This prevents thermal defects such as undercooking, overheating, and post-deposition deformation. For example, thermal imaging has been applied to observe material cooling behavior during extrusion, revealing that deformation in thermo-reversible formulations can be mitigated through appropriate parameter optimization (Ma and Zhang 2022). Concurrently, environmental humidity is monitored and controlled, as elevated moisture levels can hinder material solidification, lead to interlayer delamination, and degrade structural fidelity. Integration of real-time thermal and hygrometric monitoring enhances process stability, reduces the need for empirical calibration, and enables robust fabrication across diverse material systems. Notably, temperature and humidity not only affect the material fidelity, but also exert a direct influence on layer thickness and deposition consistency, making them critical parameters for layer-level quality control.

To further refine in-process quality assessment, a layer-wise monitoring framework was introduced by Bisheh, Chang, and Lei (2021) which utilizes top-view images and an exponentially weighted moving average chart to detect process variations during each deposition layer. This framework enables real-time identification of subtle printing anomalies by analyzing pixel-level deviations across sequential layers. In their validation experiment involving a three-inch diameter basket structure, the system successfully detected minor variations in layer geometry. Furthermore, machine learning techniques were applied to effectively separate each printed layer from the printing bed, addressing challenges posed by lighting variation.

To expand the capabilities of monitoring in 3DFP beyond surface-level defect detection, recent approaches have aimed to capture deeper structural fidelity through the integration of spatial feature analysis and digital model correlation. For instance, Armstrong et al. (2021) introduced a process evaluation framework that generates a process map coupled with material property models. This method enables the identification of feature-level deviations during printing, allowing for the quantitative assessment of spatial accuracy. Although not intended for real-time correction, the accumulated data from such monitoring schemes provide valuable insights into recurring error patterns and structural inconsistencies across different print geometries and material types.

In a similar context, vision-based monitoring has been extended to track extrusion consistency using feedback derived from visual observations. Ma et al. (2023) developed a system that dynamically analyzes the extruded material width to detect under- or over-extrusion conditions, thereby improving the accuracy of material deposition. While this approach remains focused on detection rather than actuation, it highlights the increasing role of real-time vision in identifying subtle deviations that are difficult to detect using conventional sensors.

Furthermore, Charalampous et al. (2021) proposed an advanced inspection technique for correlating physical printed parts with their original digital 3D models using high-resolution point cloud data. This method involves scanning, filtering, segmenting, and aligning the printed geometry with its corresponding CAD model, providing a comprehensive evaluation of shape conformity and dimensional accuracy. In addition to enhancing defect localization, this framework contributes to reducing production inefficiencies by minimizing feedstock material waste, labor effort, and machine time.

Despite recent advancements, a fundamental limitation remains in current 3DFP monitoring systems: the lack of a comprehensive understanding of how observed process parameters, such as layer thickness, extrusion consistency, and thermal behavior, relate to the final mechanical and structural properties of printed food constructs. This gap restricts the design flexibility and material diversity that 3DFP can accommodate, particularly when targeting complex or functionalized food products. While modern monitoring frameworks provide high-resolution, real-time sensing capabilities through vision-based, thermal, and environmental data acquisition, their diagnostic value remains limited without robust data-driven models that can translate sensor outputs into functional quality indicators such as texture, mechanical strength, and shelf-life. Addressing this challenge requires the development of predictive modeling techniques that link in-process monitoring data with end-product performance metrics. Establishing such correlations will enhance both the interpretability and utility of monitoring systems, ultimately transforming them from passive quality assessment tools into intelligent decision-support systems. In the broader context of increasingly personalized and application-driven food manufacturing, advanced monitoring technologies will play a critical role in scaling up 3DFP with reliability, precision, and industrial relevance.

4.3. Control in 3DFP

As above mentioned, sensing and monitoring methods, such as vision-based inspection and temperature measurement, have been actively studied in 3DFP. However, their integration into real-time feedback control systems remains limited. While path optimization and material flow regulation are essential for maintaining process stability and product fidelity in general 3D printing, 3DFP presents additional challenges due to the complex rheological and thermal characteristics of food materials. Most traditional 3D printing systems rely on predefined motion paths and fixed process parameters, lacking the ability to adapt to disturbances during fabrication (Ishikawa, Yamashita, and Tasaki 2023).

Real-time feedback control in 3DFP utilizes sensor data and monitoring systems to dynamically adjust the printing process in response to deviations. To improve extrusion accuracy in pneumatic 3DFP systems, Ma et al. (2023) proposed a feed-forward control strategy that adjusts nozzle motion based on real-time measurements of extrusion speed and filament width. These parameters were obtained using visual observations. The proposed control strategy of printing achieved accuracy ranged from 97.9 to 100%. Compared to constant printing, the calibrated printing improved the length accuracy ranging from 4.7 to 10.6%. However, the primary objective of the method is not quality inspection

but motion adaptation under constant extrusion pressure or force. This approach enhances initial motion planning but still lacks the dynamic adaptability required to compensate for real-time variations in material behavior during printing.

Another important aspect of control in 3DFP is the regulation of nutritional content through digital management of food composition. By adjusting material density and deposition strategies, it is possible to fabricate customized food products with targeted ingredient distribution, texture, and structural characteristics to meet specific dietary requirements (Sun et al. 2018). While the concept of personalized nutrition through 3DFP holds considerable potential, practical implementation remains limited, highlighting the need for further research in process control and material formulation strategies. Yoha et al. (2021) demonstrated that 3D printing of synbiotic-composite foods preserved 98–99% of encapsulated probiotics, representing a clear improvement over free-cell survival (~70%). The ability to control internal structure and surface-to-volume ratio during printing contributed to more effective protection and integration of probiotics within the food matrix. The combination of spray freeze-drying encapsulation and freeze-drying resulted in the highest viability after digestion (6.43 $\log_{10}$ CFU/mL) and 94% retention during storage, suggesting that 3D food printing can enhance the nutritional value of functional foods by improving the delivery and retention of bioactive ingredients. Liu, Bhandari, and Zhang (2020) investigated 3DFP of mashed potatoes and found that extrusion and structural stability were governed by rheological properties such as yield stress and elastic modulus. Probiotic viability remained high under most conditions, with only a slight decrease when using a 0.6 mm nozzle (from 9.93 to 9.74 log CFU/g) and a larger reduction after exposure to 55 °C for 45 min (from 10.07 to 7.99 log CFU/g). All samples maintained viability above 9.7 log CFU/g during 12-day storage, confirming that 3DFP can produce probiotic-enriched foods when formulation and thermal exposure are carefully managed.

Flow rate control in 3D printing is critical for mitigating defects caused by under- or over-extrusion, which can adversely affect the structural and esthetic quality of printed food products. Traditional approaches have largely relied on adjusting print speed to manage flow inconsistencies; however, such methods often yield limited improvements in printing accuracy. To address this limitation, Brion & Pattinson proposed a system that directly utilizes flow parameters for printer control, as illustrated in Figure 5(a) (Brion and Pattinson 2022b). By treating flow rate as a continuous variable, their approach enables more precise prediction and adjustment of flow conditions, resulting in faster response times and improved printing performance. During the printing process, an event was introduced that reduced the material flow rate to 50% of its optimal value (from 3.60 to 1.80 mm^3/s). In the absence of feedback control, this disturbance led to severe under-extrusion and significant degradation in the printed product. In contrast, when the proposed few-shot control system was applied, it accurately detected the error and predicted the necessary correction. The flow rate was promptly adjusted, resulting in stable material deposition and improved print quality. Although the system's performance was not quantitatively evaluated, qualitative observations confirmed its effectiveness in recovering from severe flow disturbances.

While single-parameter control can enhance local performance, it remains insufficient for maintaining overall process stability. In a subsequent study, Brion and Pattinson developed a multi-head neural network trained on image datasets that were automatically labeled based on deviations from optimal printing conditions, as illustrated in Figure 5(b) (Brion and Pattinson 2022a). This architecture enables multi-parameter learning and contributes to the simultaneous optimization of several process variables. Based on this framework, a real-time correction pipeline was implemented. Operating at 2.5 Hz, the system classifies printing conditions such as under-extrusion, over-extrusion, and acceptable deposition, and applies proportional corrections to parameters including flow rate, Z offset, hotend temperature, and lateral speed. The system demonstrated the capability to recover unstable prints by restoring consistent material deposition across various printers, geometries, and materials. Qualitative evaluations further confirmed improved surface quality and higher success rates, even under initially incorrect parameter settings, thereby validating the practical utility of multi-parameter control in real-world 3DFP applications. In a related study, Jin, Zhang, and Gu (2019) developed an autonomous FDM platform that integrates machine learning for real-time monitoring and adaptive control of printing conditions. The platform achieved over 98% accuracy in predicting print quality and outperformed human evaluators in detecting subtle visual defects, as shown in Figure 5(c).

Tamir et al. (2023) proposed a closed-loop control framework for additive manufacturing that integrates a fuzzy logic–based feedback system with a mathematical model of the 3D printer to optimize four key processing parameters. The fuzzy system continuously monitors the printing process through rule-based inference, dynamically adjusting parameters in real time to maintain consistent part quality. Building on this foundation, the authors further extended their framework by incorporating both open-loop and closed-loop machine learning models. A fuzzy inference mechanism was used to combine predictive outputs with real-time feedback, enabling more refined control decisions and leading to improved functional properties of printed parts (Figure 5(d)). This work represents one of the first implementations of a fully closed-loop, machine learning–driven control strategy in 3D printing.

In summary, while the integration of advanced control strategies with machine learning techniques shows considerable promise for addressing the inherent complexities of 3DFP, most existing studies remain focused on developing the control methodology itself rather than quantitatively evaluating printability or final product quality. Furthermore, the majority of demonstrations have been conducted on conventional thermoplastic-based 3D printing platforms rather than food-specific systems. Due to the thermally sensitive and highly variable nature of food inks, implementing real-time control in 3DFP poses additional challenges. As such, there remains a significant gap in the literature

regarding validated, real-time control frameworks tailored to food printing applications, indicating a critical need for further research in this domain.

5. Future perspectives

For intelligent 3DFP, integrated considerations are required with respect to materials, fabrication, monitoring, and control of 3DFP. In intelligent 3DFP materials, future research should focus on the development of innovative materials, diversification of food sources, a deeper understanding of interactions in multi-material system, and design customized materials.

To fully harness the potential of 4DFP, the integration of dynamic materials with intelligent 3DFP systems is essential. While stimulation was typically applied to a separate device after printing, intelligent 3DFP systems can be integrated with on-board stimulation modules such as UV, infrared, laser, microwave, or thermal units enabling precise control of material responses during and immediately after the printing process (Fujiwara et al. 2025; Kocaman, Bulut, and Özcan 2025; Xiao et al. 2025). This integration allows for real-time, localized application of external stimuli, facilitating on-demand transformations including shape deformation, color change, or nutrient activation (Navaf et al. 2022). Therefore, intelligent 3DFP systems ensure that printed structures are fabricated with high dimensional accuracy, reducing the risk of printing failure and enabling predictable, targeted post-printing shape changes. By leveraging real-time material monitoring data, these systems can also optimize stimulus parameters to achieve desired transformations in color, texture, or nutritional content with greater precision and efficiency.

Meanwhile, living materials, such as cell-based bioinks, incorporate viable cells within the printing matrix, allowing for biological activity, tissue development, and even metabolic functions post-printing, as seen in the production of cultivated meat and cell-based foods. Intelligent 3DFP systems provide a promising platform for these applications by enabling precise control over the printing environment (e.g., temperature, humidity, oxygen), real-time monitoring of cell behavior, and adaptive feedback to optimize cell viability, growth, and differentiation. These systems can be integrated with embedded biosensors to analyze cellular responses during and after printing, adjusting environmental parameters accordingly. This approach enables continuous, multiplexed monitoring of metabolic conditions across the printed structure in real time, without disrupting cell viability or print fidelity. By integrating the biosensing platforms such as oxygen-sensitive microsensors (Iuele et al. 2024) and multiplexed metabolic reporters (Saleem et al. 2025) with intelligent 3DFP systems can leverage real-time, noninvasive monitoring to dynamically adjust environmental conditions and printing parameters. This could pave the way for cell-based food production by ensuring optimal cell viability and functional fidelity of the printed structures.

Moreover, the diversity of food sources will remain essential in future food design, as material interactions affect texture, stability, taste, and digestibility. In addition to personal health and preference customization, sustainability is also a key focus for the future of 3DFP (Wu, Zhu, and Li 2024). To ensure both diversity and sustainability, precision fermentation based on synthetic biology could be a promising solution (Hilgendorf et al. 2024). The technology can leverage metabolic engineering tools to produce a variety of food ingredients, including carbohydrates, proteins, lipids, and flavors, which can affect the printability of food ink in 3DFP. For instance, precision fermentation enables the production of a specific type of animal-free protein (i.e., β-lactoglobulin, α-lactoalbumin, and β-casein) (Jin, Seo, and Kim 2024). By adjusting the composition or concentration of these proteins, it is possible to enhance the solubility of food inks, leading to better printability for dairy products in 3DFP, compared to traditional cow milk-based inks. Therefore, it is crucial to investigate further the printability and nutritional profiles of food materials produced through precision fermentation in 3DFP as well as in advanced printing techniques (i.e., 4D, 5D, and 6D printing) for a more comprehensive understanding and development. For commercial production, building social consensus is also critical, as regulatory issues surrounding LMOs and GMOs remain a significant challenge.

Toward creating more complex and heterogeneous food structures, interfacial design and material compatibility in multi-material 3DFP is important. Multi-material 3DFP introduces an additional layer of complexity the interactions at the interfaces between distinct inks. Unlike homogeneous printing, co-deposition of multiple inks such as starch-based pastes and protein gels requires that their respective physicochemical properties be not only independently tunable but also mutually compatible. Thus, a deeper understanding of the interfacial bonding mechanisms such as hydrogen bonding, electrostatic interaction, or diffusion-based entanglement between different materials is critical to ensuring cohesive structure formation. Recent multi-material research highlight the promise of composite ink systems, but also point to the challenges in achieving consistent interface adhesion and deformation response across material boundaries (Ahmadzadeh and Ubeyitogullari 2024; Lenie et al. 2024). Future research should therefore focus on mapping the physicochemical interactions at the ink–ink interface, assessing how these impacts the overall rheology, structural integration, and stimuli-responsiveness of the printed constructs. This approach will be essential for the development of reliable and high-performance multi-material 3DFP systems, especially within the context of intelligent 3DFP systems, where real-time control further amplifies the need for interface stability.

To better address the potential of 3DFP in personalized nutrition, future research should explore food ink formulations tailored to the physiological needs of specific population groups, while also accounting for regional accessibility and economic feasibility. For example, diabetic individuals may benefit from low-glycemic inks using resistant starch, dietary fibers, and non-glycemic sweeteners (Huang et al. 2024). However, practical limitations such as the high cost of bio-functional ingredients, limited availability of printing

hardware, and infrastructure disparities across regions may challenge widespread implementation (Lee 2021; Varvara, Szabo, and Vodnar 2021). Therefore, material innovation should also consider scalable, low-cost ingredients and simplified printing systems suitable for diverse settings. Beyond clinical and household applications, 3DFP holds promise for the food service industry by enabling on-demand customization of meals in restaurants, catering services, and institutional kitchens, offering flexibility in portioning, esthetics, and nutrient composition. Collectively, these considerations position intelligent 3DFP not only as a tool for medical and personalized nutrition but also as a versatile platform for broader food system innovation. In terms of environmental sustainability, 3DFP contributes to food waste reduction by enabling precise portion control, utilizing upcycled ingredients, and facilitating on-demand production, which minimizes spoilage and overproduction. For future research, it is important to evaluate the actual impact of 3DFP on food waste reduction.

Conventional 3D printing technologies can overcome existing limitations through the integration of new devices or the combination of different processes. For instance, equipping an extrusion-based 3D printer with a laser irradiation module enables real-time modulation of ink properties during deposition, potentially eliminating the need for post-printing cooking. Additionally, hybridizing binder jetting with extrusion-based printing can significantly reduce nozzle travel distance during infill processes and facilitate the fabrication of multi-material food structures, which is typically challenging in binder jetting alone. Such hybrid printing approaches require precise coordination between slicers, food modeling software, and printer control systems. Incorporating predictive capabilities into slicer software, particularly those that can simulate inter-material bonding and rheological behavior during the material design stage, can improve both structural stability and printing resolution. When these predictive design systems are integrated with real-time monitoring and control modules, a closed-loop feedback system can be established. This system can compare simulated outputs with actual print data, enabling automatic error correction or adaptive process parameter adjustments. These advancements lay the foundation for the realization of intelligent food 3D printing systems.

However, in the context of food printing, the functional requirements of advanced 3D printers differ significantly from conventional applications due to the inherently multi-ingredient nature of most food products. For example, reproducing a steak involves spatially organized deposition of multiple components such as muscle and fat, making multi-material printing essential. While powder-based methods like binder jetting and SLS offer benefits such as support-less fabrication and high geometric complexity, they are generally unsuitable for multi-material food printing because precise spatial control of different edible ingredients is difficult. These techniques may still be useful in fabricating functional foods with materials not suited for extrusion, but their applicability to realistic food structuring remains limited. Once multi-material capabilities are established, 3DFP systems can produce complex architectures including marbling patterns in meat, core–shell structures, and novel infill designs, enabling textures unattainable by conventional methods. Additionally, multi-material printing can address challenges in support removal, a common limitation in extrusion-based printing. Strategies inspired by industrial printing, such as water-soluble or thermally responsive supports, could be adapted so that structural components harden during cooking while temporary supports dissolve. Although such advancements enhance the design freedom of 3DFP and partially mitigate constraints imposed by food ink rheology, further progress toward ultra-high-resolution or 4DFP is still limited by fundamental material properties.

Alongside the hardware advancements discussed earlier, such as multi-material deposition and complex geometry fabrication, these material limitations highlight the need for more precise and adaptive process control. The structural complexity introduced by multi-material deposition and functional layering in 3DFP necessitates precise control to maintain geometric accuracy and material consistency. Although sensing and monitoring technologies have progressed, their integration into real-time feedback control remains limited. High-precision tasks such as printing with multiple materials or complex geometries require continuous adjustment of parameters including extrusion rate, nozzle movement, and layer alignment. These adjustments must respond to dynamic variations in material behavior, temperature, and environmental conditions. Accurate coordination between sensor feedback and actuator response is essential to prevent defects such as misalignment and surface inconsistency, thereby improving structural integrity, surface quality, and sensory attributes. Traditional feedforward control, which lacks feedback from the printed output, cannot accommodate such variability. Therefore, reliable material deposition under varying conditions necessitates closed-loop control systems that adapt in real time.

To address these challenges, model predictive control (MPC) and learning-based methods offer effective solutions for improving adaptability. MPC enables real-time optimization based on current sensor input, allowing prediction and correction of future deviations. Learning-based approaches, including reinforcement learning, refine control policies over time by evaluating past performance, enabling the system to handle previously unseen disturbances. These methods allow dynamic adjustment of extrusion rate, nozzle trajectory, and thermal input in response to variations in viscosity, deformation, or temperature. When combined with AI-driven decision-making, they support real-time parameter tuning and fault recovery. Digital twin technology further enhances system robustness by providing a virtual replica of the printing process for predictive diagnostics and simulation. Together, these technologies enable the development of intelligent 3DFP systems capable of adapting to complex and variable printing scenarios.

While this review primarily addresses the technical foundations of intelligent 3DFP systems, it is also important to consider broader interdisciplinary implications including food culture, consumer acceptance, and socioeconomic impact. From a functional standpoint, personalized food manufacturing based on individual dietary profiles presents

high potential in healthcare and performance-oriented domains. However, such customization inherently introduces production inefficiencies and increased cost per unit, limiting its viability in conventional supply chains (Baiano 2022). 3DFP provides a structured approach to mitigate these limitations through automation and modular design, enabling cost-effective production of complex and customized food geometries at scale. Nonetheless, integration into real-world applications remains constrained by limited consumer acceptance, particularly with regard to novel ingredients such as cell-cultured proteins or texturized analogs. According to survey (Lupton and Turner 2018) indicate that end users often associate such products with artificiality and uncertainty in safety, nutrition, and taste. To support deployment in practical food systems, 3DFP must be aligned with standardized labeling protocols, material traceability, and validated safety regulations. These components, in conjunction with technical maturity, will facilitate the transition from laboratory-scale demonstrations to consumer-facing platforms and enhance system-level acceptance across diverse demographic and regulatory contexts. Also, the scalability and commercial viability of 3DFP remain limited due to constraints such as slow production speed, lack of standardized food ink formulations, high equipment costs, consumer acceptance challenges, and complex regulatory approval processes, particularly for novel bioengineered ingredients. These limitations highlight the need for more comprehensive investigation and strategic planning to ensure the scalability and commercial viability of 3DFP technologies.

6. Conclusions

This review highlighted the crucial elements of intelligent 3DFP, including materials, fabrication methods, and sensing and control systems. Edible and printable materials should exhibit excellent printability, characterized by sufficient extrudability and self-supporting ability. Integrated sensing, monitoring, and control systems offer opportunities to overcome current limitations in 3DFP. In the intelligent 3DFP, the quality and adaptability of 3DFP can be improved by developing robust real-time feedback systems, enhancing the understanding of material behavior, and optimizing multiple parameters simultaneously. Based on the proposed intelligent 3DFP system, food can be customized with high accuracy for specific purposes, making it valuable and applicable in diverse fields, such as combat rations and healthcare.

Author contributions

Writing draft including figures and tables: J. Seol, J. Kim, M. Cha and Y. Hong; Conceptualization: S. Park, KJ. Jang, SJ. Kim, and H. I. Son; Literature search through scientific data-bases: J. Seol, J. Kim, M. Cha and Y. Hong; Revised manuscript: J. Seol and all authors.

Disclosure statement

No potential conflict of interest was reported by the author(s).

Funding

This work was supported by a National Research Foundation of Korea (NRF) grant funded by the Korea government (MSIT) (No. NRF-2023R1A2C1003701). Also, this work was supported by Korea Institute of Planning and Evaluation for Technology in Food, Agriculture and Forestry (IPET) through Agriculture and Food Convergence Technologies Program for Research Manpower development, funded by Ministry of Agriculture, Food and Rural Affairs (MAFRA) (RS-2024–00397026 and RS-2024–00402136). This work was supported by the fund of research promotion program, Gyeongsang National University 2020.

References

Ahmadzadeh, S., and A. Ubeyitogullari. 2024. Lutein encapsulation into dual-layered starch/zein gels using 3D food printing: Improved storage stability and in vitro bioaccessibility. *International Journal of Biological Macromolecules* 266, Part 2,131305–15. doi: 10.1016/j.ijbiomac.2024.131305.

Alam, M., M. Rawat, S. Kaur, B. N. Dar, and V. Nanda. 2024. Transformation of quality attributes of fruit leathers using diverse hydrocolloids: Recent application and future perspective. *Journal of Food Process Engineering* 47 (11): E14782–800. doi: 10.1111/jfpe.14782.

Alzyod, H., and P. Ficzere. 2023. Material-dependent effect of common printing parameters on residual stress and warpage deformation in 3D printing: A comprehensive finite element analysis study. *Polymers* 15 (13):2893–912. doi: 10.3390/polym15132893.

Armstrong, A. A., A. Pfeil, A. G. Alleyne, and A. J. W. Johnson. 2021. Process monitoring and control strategies in extrusion-based bioprinting to fabricate spatially graded structures. *Bioprinting* 21: E00126–35. doi: 10.1016/j.bprint.2020.e00126.

Armstrong, C. D., L. Yue, Y. Deng, and H. J. Qi. 2022. Enabling direct ink write edible 3D printing of food purees with cellulose nanocrystals. *Journal of Food Engineering* 330:111086–92. doi: 10.1016/j.jfoodeng.2022.111086.

Aydin, G., B. C. Sarar, M. E. Yildizdag, and B. E. Abali. 2022. Investigating infill density and pattern effects in additive manufacturing by characterizing metamaterials along the strain-gradient theory. *Mathematics and Mechanics of Solids* 27 (10):2002–16. doi: 10.1177/10812865221100978.

Baiano, A. 2022. 3D printed foods: A comprehensive review on technologies, nutritional value, safety, consumer attitude, regulatory framework, and economic and sustainability issues. *Food Reviews International* 38 (5):986–1016. doi: 10.1080/87559129.2020.1762091.

Bakhsh, A., B. Kim, I. Ishamri, S. Choi, X. Li, Q. Li, S. J. Hur, and S. Park. 2025. Cell-based meat safety and regulatory approaches: A comprehensive review. *Food Science of Animal Resources* 45 (1):145–64. doi: 10.5851/kosfa.2024.e122.

Bao, C., H. Moeinnia, T. Kim, W. Lee, and W. S. Kim. 2023. 3D structural electronics via multi-directional robot 3D printing. *Advanced Materials Technologies* 8 (5):2201349–57. doi: 10.1002/admt.202201349.

Bao, Y., T. Yang, and H. Jiang. 2024. Effect of 3D printing accuracy by wheat starch gel combined with canola oil. *International Journal of Biological Macromolecules* 282 (Pt 1):136614–24. doi: 10.1016/j.ijbiomac.2024.136614.

Bian, M., S. Jiang, S. Liu, L. Zhang, S. Miao, F. Zhou, and B. Zheng. 2024. Fish gelatin and gellan gum mixture as edible ink for 3D printing. *Journal of Food Engineering* 362:111762–70. doi: 10.1016/j.jfoodeng.2023.111762.

Bisheh, M. N., S. I. Chang, and S. Lei. 2021. A layer-by-layer quality monitoring framework for 3D printing. *Computers & Industrial Engineering* 157:107314–25. doi: 10.1016/j.cie.2021.107314.

Blutinger, J. D., A. Tsai, E. Storvick, G. Seymour, E. Liu, N. Samarelli, S. Karthik, Y. Meijers, and H. Lipson. 2021. Precision cooking for printed foods via multiwavelength lasers. *NPJ Science of Food* 5 (1):24–32. doi: 10.1038/s41538-021-00107-1.

Brion, D. A. J., and S. W. Pattinson. 2022b. Quantitative and real-time control of 3d printing material flow through deep learning. *Advanced Intelligent Systems* 4 (11):2200153–62. doi: 10.1002/aisy.202200153.

Brion, D. A., and S. W. Pattinson. 2022a. Generalisable 3D printing error detection and correction via multi-head neural networks. *Nature Communications* 13 (1):4654–67. doi: 10.1038/s41467-022-31985-y.

Cai, N., X. N. Chen, W. C. Ou, Z. Y. X. Wu, G. F. Zheng, H. Wang, and J. Zeng. 2024. Error analysis and correction for electrohydrodynamic printing: A review. *3D Printing and Additive Manufacturing* :1–24. doi: 10.1089/3dp.2023.0313.

Carvajal-Mena, N., G. Tabilo-Munizaga, M. Pérez-Won, and R. Lemus-Mondaca. 2022. Valorization of salmon industry by-products: Evaluation of salmon skin gelatin as a biomaterial suitable for 3D food printing. *Lwt* 155:112931–41. doi: 10.1016/j.lwt.2021.112931.

Chadwick, E., A. H. Barrett, M. Okamoto, Y. Suleiman, G. P. S. R. Bertola, S. Shahbazmohamadi, A. Shetty, Y. H. Li, and A. W. K. Ma. 2024. Binder-jet 3D printing of pea-based snacks with modulated texture. *Journal of Food Engineering* 378:112112–21. doi: 10.1016/j.jfoodeng.2024.112112.

Chadwick, E., G. P. S. R. Bertola, X. H. Lin, A. H. Barrett, M. Okamoto, X. L. Lu, and A. W. K. Ma. 2025. 3D printing fortified pea-based snacks with precise vitamin dosing by binder jetting. *Journal of Food Engineering* 391:112465–74. doi: 10.1016/j.jfoodeng.2024.112465.

Chandimali, N., E. H. Park, S. Bak, Y. Won, H. Lim, and S. Lee. 2024. Not seafood but seafood: A review on cell-based cultured seafood in lieu of conventional seafood. *Food Control.* 162:110472–9. doi: 10.1016/j.foodcont.2024.110472.

Charalampous, P., I. Kostavelis, T. Kontodina, and D. Tzovaras. 2021. Learning-based error modeling in FDM 3D printing process. *Rapid Prototyping Journal* 27 (3):507–17. doi: 10.1108/RPJ-03-2020-0046.

Charoo, N. A., S. F. B. Ali, E. M. Mohamed, M. A. Kuttolamadom, T. Ozkan, M. A. Khan, and Z. Rahman. 2020. Selective laser sintering 3D printing–An overview of the technology and pharmaceutical applications. *Drug Development and Industrial Pharmacy* 46 (6):869–77. doi: 10.1080/03639045.2020.1764027.

Chen, H., F. Xie, L. Chen, and B. Zheng. 2019. Effect of rheological properties of potato, rice and corn starches on their hot-extrusion 3D printing behaviors. *Journal of Food Engineering* 244:150–8. doi: 10.1016/j.jfoodeng.2018.09.011.

Chen, J., M. Zhang, and S. Devahastin. 2021. UV-C irradiation-triggered nutritional change of 4D printed ergosterol-incorporated purple sweet potato pastes: Conversion of ergosterol into vitamin D2. *Lwt* 150:111944–51. doi: 10.1016/j.lwt.2021.111944.

Chen, Y., D. J. McClements, X. Peng, L. Chen, Z. Xu, M. Meng, X. Zhou, J. Zhao, and X. Jin. 2024. Starch as edible ink in 3D printing for food applications: A review. *Critical Reviews in Food Science and Nutrition* 64 (2):456–71. doi: 10.1080/10408398.2022.2106546.

Cheng, Y., K. Liang, Y. Chen, W. Gao, X. Kang, T. Li, and B. Cui. 2023. Effect of molecular structure changes during starch gelatinization on its rheological and 3D printing properties. *Food Hydrocolloids.* 137:108364–72. doi: 10.1016/j.foodhyd.2022.108364.

Chung, H., T. W. Kim, M. Kwon, I. C. Kwon, and S. Y. Jeong. 2001. Oil components modulate physical characteristics and function of the natural oil emulsions as drug or gene delivery system. *Journal of Controlled Release: Official Journal of the Controlled Release Society* 71 (3):339–50. doi: 10.1016/S0168-3659(00)00363-1.

Co, E. D., and A. G. Marangoni. 2018. Oleogels: An introduction. In *Edible oleogels*: Structure and Health Implications, ed. A. G. Marangoni and N. Garti, 1–29. Urbana, IL: AOCS PRESS. doi: 10.1016/B978-0-12-814270-7.00001-0.

Colucci, G., F. Lupone, F. Bondioli, and M. Messori. 2024. 3D printing of PBAT-based composites filled with agro-wastes via selective laser sintering. *European Polymer Journal* 215:113197–209. doi: 10.1016/j.eurpolymj.2024.113197.

Cortez-Trejo, M. C., M. Gaytán-Martínez, M. L. Reyes-Vega, and S. Mendoza. 2021. Protein-gum-based gels: Effect of gum addition on microstructure, rheological properties, and water retention capacity. *Trends in Food Science & Technology* 116:303–17. doi: 10.1016/j.tifs.2021.07.030.

Daffner, K., S. Vadodaria, L. Ong, S. Nöbel, S. Gras, I. Norton, and T. Mills. 2021. Design and characterization of casein–whey protein suspensions via the pH–temperature-route for application in extrusion-based 3D-Printing. *Food Hydrocolloids.* 112:105850–8. doi: 10.1016/j.foodhyd.2020.105850.

Dankar, I., A. Haddarah, F. E. Omar, F. Sepulcre, and M. Pujolà. 2018. 3D printing technology: The new era for food customization and elaboration. *Trends in Food Science & Technology* 75:231–42. doi: 10.1016/j.tifs.2018.03.018.

Delli, U., and S. Chang. 2018. Automated process monitoring in 3D printing using supervised machine learning. *Procedia Manufacturing* 26:865–70. doi: 10.1016/j.promfg.2018.07.111.

Duty, C., C. Ajinjeru, V. Kishore, B. Compton, N. Hmeidat, X. Chen, P. Liu, A. A. Hassen, J. Lindahl, and V. Kunc. 2018. What makes a material printable? A viscoelastic model for extrusion-based 3D printing of polymers. *Journal of Manufacturing Processes* 35:526–37. doi: 10.1016/j.jmapro.2018.08.008.

El Moumen, A., M. Tarfaoui, and K. Lafdi. 2019. Modelling of the temperature and residual stress fields during 3D printing of polymer composites. *The International Journal of Advanced Manufacturing Technology* 104 (5-8):1661–76. doi: 10.1007/s00170-019-03965-y.

Fan, F., S. Li, W. Huang, and J. Ding. 2022. Structural characterization and fluidness analysis of lactose/whey protein isolate composite hydrocolloids as printing materials for 3D printing. *Food Research International (Ottawa, Ont.)* 152:110908–17. doi: 10.1016/j.foodres.2021.110908.

Fan, M., Y. Choi, N. E. Wedamulla, S. Kim, S. M. Bae, D. Yang, H. Kang, Y. Tang, S. Moon, and E. Kim. 2024. Different particle sizes of Momordica charantia leaf powder modify the rheological and textural properties of corn starch-based 3D food printing ink. *Heliyon* 10 (4):e24915-27. doi: 10.1016/j.heliyon.2024.e24915.

Fujiwara, K., Y. Igeta, K. Toba, J. Ogawa, H. Furukawa, M. Hashizume, T. Noji, K. Teratani, and N. Ito. 2025. Laser cook fusion: Layer-specific gelation in 3D food printing via blue laser irradiation. *Food and Bioprocess Technology* 18 (7):6265–81. doi: 10.1007/s11947-025-03817-6.

Gao, H., L. Ma, C. Cheng, J. Liu, R. Liang, L. Zou, W. Liu, and D. J. McClements. 2021. Review of recent advances in the preparation, properties, and applications of high internal phase emulsions. *Trends in Food Science & Technology* 112:36–49. doi: 10.1016/j.tifs.2021.03.041.

Geng, M., T. Hu, Q. Zhou, A. Taha, L. Qin, W. Lv, X. Xu, S. Pan, and H. Hu. 2021. Effects of different nut oils on the structures and properties of gel-like emulsions induced by ultrasound using soy protein as an emulsifier. *International Journal of Food Science & Technology* 56 (4):1649–60. doi: 10.1111/ijfs.14786.

Glicksman, M. 2020. Functional properties of hydrocolloids. In *Food hydrocolloids*, ed. M. Glicksman, 47–99. New York:Routledge.

Godoi, F. C., S. Prakash, and B. R. Bhandari. 2016. 3d printing technologies applied for food design: Status and prospects. *Journal of Food Engineering* 179:44–54. doi: 10.1016/j.jfoodeng.2016.01.025.

Gu, M., H. Gu, V. Raghavan, and J. Wang. 2024. Ultrasound treatment improved the physicochemical properties of pea protein with pectin ink used for 3D printing. *Future Foods* 9:100377–85. doi: 10.1016/j.fufo.2024.100377.

Gugliandolo, S. G., A. Margarita, S. Santoni, D. Moscatelli, and B. M. Colosimo. 2022. In-situ monitoring of defects in extrusion-based bioprinting processes using visible light imaging. *Procedia CIRP* 110:219–24. doi: 10.1016/j.procir.2022.06.040.

Guo, C., M. Zhang, and B. Bhandari. 2019. Model building and slicing in food 3D printing processes: A review. *Comprehensive Reviews in Food Science and Food Safety* 18 (4):1052–69. doi: 10.1111/1541-4337.12443.

Guo, Y., H. S. Patanwala, B. Bognet, and A. W. K. Ma. 2017. Inkjet and inkjet-based 3D printing: Connecting fluid properties and printing performance. *Rapid Prototyping Journal* 23 (3):562–76. doi: 10.1108/RPJ-05-2016-0076.

Han, N., J. Bae, H. W. An, H. Yun, B. Retnoaji, S. Lee, and S. G. Lee. 2025. Influence of potato starch on the 3D printing of senior-friendly foods enriched with oyster powder. *LWT* 224:117886–94. doi: 10.1016/j.lwt.2025.117886.

Hassan, I., N. Rasheed, A. Gani, and A. Gani. 2025. Rice starch, millet flour supplemented with algal biomass for 3D food printing. *International Journal of Biological Macromolecules* 303:140604–16. doi: 10.1016/j.ijbiomac.2025.140604.

He, C., M. Zhang, and C. Guo. 2020. 4D printing of mashed potato/purple sweet potato puree with spontaneous color change. *Innovative Food Science & Emerging Technologies* 59:102250–64. doi: 10.1016/j.ifset.2019.102250.

He, C., M. Zhang, and Z. Fang. 2020. 3D printing of food: Pretreatment and post-treatment of materials. *Critical Reviews in Food Science and Nutrition* 60 (14):2379–92. doi: 10.1080/10408398.2019.1641065.

Hilgendorf, K., Y. Wang, M. J. Miller, and Y. Jin. 2024. Precision fermentation for improving the quality, flavor, safety, and sustainability of foods. *Current Opinion in Biotechnology* 86:103084–92. doi: 10.1016/j.copbio.2024.103084.

Holland, S., C. Tuck, and T. Foster. 2018. Selective recrystallization of cellulose composite powders and microstructure creation through 3D binder jetting. *Carbohydrate Polymers* 200:229–38. doi: 10.1016/j.carbpol.2018.07.064.

Hu, X., Q. Jiang, L. Du, and Z. Meng. 2023. Edible polysaccharide-based oleogels and novel emulsion gels as fat analogues: A review. *Carbohydrate Polymers* 322:121328–46. doi: 10.1016/j.carbpol.2023.121328.

Huang, J., M. Zhang, A. S. Mujumdar, and C. Li. 2024. Modulation of starch structure, swallowability and digestibility of 3D-printed diabetic-friendly food for the elderly by dry heating. *International Journal of Biological Macromolecules* 264 (Pt 2):130629–43. doi: 10.1016/j.ijbiomac.2024.130629.

Hussain, S., S. Malakar, and V. K. Arora. 2022. Extrusion-based 3D food printing: Technological approaches, material characteristics, printing stability, and post-processing. *Food Engineering Reviews* 14 (1):100–19. doi: 10.1007/s12393-021-09293-w.

Impens, D., and R. J. Urbanic. 2016. A comprehensive assessment on the impact of post-processing variables on tensile, compressive and bending characteristics for 3D printed components. *Rapid Prototyping Journal* 22 (3):591–608. doi: 10.1108/RPJ-02-2015-0018.

Ishikawa, S., T. Yamashita, and R. Tasaki. 2023. Vision-based monitoring and control for 3D printing process with dynamic ROI and path modification algorithm. *Journal of Advances in Information Technology* 14 (6):1443–9. doi: 10.12720/jait.14.6.1443-1449.

Iuele, H., S. Forciniti, V. Onesto, F. Colella, A. C. Siciliano, A. Chandra, C. Nobile, G. Gigli, and L. L. del Mercato. 2024. Facile one pot synthesis of hybrid core–shell silica-based sensors for live imaging of dissolved oxygen and hypoxia mapping in 3D cell models. *ACS Applied Materials & Interfaces* 16 (41):55071–85. doi: 10.1021/acsami.4c08306.

Ji, X., J. Liang, J. Liu, J. Shen, Y. Li, Y. Wang, C. Jing, S. A. Mabury, and R. Liu. 2023. Occurrence, fate, human exposure, and toxicity of commercial photoinitiators. *Environmental Science & Technology* 57 (32):11704–17. doi: 10.1021/acs.est.3c02857.

Jiang, Q., B. P. Binks, and Z. Meng. 2022. Double scaffold networks regulate edible Pickering emulsion gel for designing thermally actuated 4D printing. *Food Hydrocolloids*. 133:107969–78. doi: 10.1016/j.foodhyd.2022.107969.

Jin, K. C., S. Seo, and S. Kim. 2024. Animal-free production of hen egg ovalbumin in engineered Saccharomyces cerevisiae via precision fermentation. *International Journal of Biological Macromolecules* 271 (Pt 1):132479–85. doi: 10.1016/j.ijbiomac.2024.132479.

Jin, Z., Z. Zhang, and G. X. Gu. 2019. Autonomous in-situ correction of fused deposition modeling printers using computer vision and deep learning. *Manufacturing Letters* 22:11–5. doi: 10.1016/j.mfglet.2019.09.005.

Jonkers, N., J. V. Dommelen, and M. G. D. Geers. 2022. An anisotropic elasto-viscoplastic-damage model for selective laser sintered food. *Engineering Fracture Mechanics* 266:108368–86. doi: 10.1016/j.engfracmech.2022.108368.

Kadival, A., J. Mitra, R. Machavaram, and M. Kaushal. 2024. 3D printing of rice starch incorporated peanut protein isolate paste: Rheological characterization and simulation of flow properties. *Innovative Food Science & Emerging Technologies* 94:103669–80. doi: 10.1016/j.ifset.2024.103669.

Kadival, A., M. Kour, D. Meena, and J. Mitra. 2023. Extrusion-based 3D food printing: Printability assessment and improvement techniques. *Food and Bioprocess Technology* 16 (5):987–1008. doi: 10.1007/s11947-022-02931-z.

Kang, D.-H., F. Louis, H. Liu, H. Shimoda, Y. Nishiyama, H. Nozawa, M. Kakitani, D. Takagi, D. Kasa, E. Nagamori, et al. 2021. Engineered whole cut meat-like tissue by the assembly of cell fibers using tendon-gel integrated bioprinting. *Nature Communications* 12 (1):5059–70. doi: 10.1038/s41467-021-25236-9.

Kang, S. W, and J. Mueller. 2024. Multiscale 3D printing via active nozzle size and shape control. *Science Advances* 10 (23):eadn7772. doi: 10.1126/sciadv.adn7772.

Karna, N. B. A., M. A. P. Putra, S. M. Rachmawati, M. Abisado, and G. A. Sampedro. 2023. Toward accurate fused deposition modeling 3d printer fault detection using improved YOLOv8 with hyperparameter optimization. *IEEE Access.* 11:74251–62. doi: 10.1109/ACCESS.2023.3293056.

Kavimughil, M., M. M. Leena, J. A. Moses, and C. Anandharamakrishnan. 2022. Effect of material composition and 3D printing temperature on hot-melt extrusion of ethyl cellulose based medium chain triglyceride oleogel. *Journal of Food Engineering* 329:111055–64. doi: 10.1016/j.jfoodeng.2022.111055.

Khan, M. F., A. Alam, M. A. Siddiqui, M. S. Alam, Y. Rafat, N. Salik, and I. Al-Saidan. 2021. Real-time defect detection in 3D printing using machine learning. *Materials Today: Proceedings* 42:521–8. doi: 10.1016/j.matpr.2020.10.482.

Khan, S. A., X. Ma, S. V. Jermain, H. Ali, I. A. Khalil, M. E. Fouly, A. H. Osman, and R. O. Williams. III. 2022. Sustained release biocompatible ocular insert using hot melt extrusion technology: Fabrication and in-vivo evaluation. *Journal of Drug Delivery Science and Technology* 71:103333–43. doi: 10.1016/j.jddst.2022.103333.

Kim, H. W., H. Bae, and H. J. Park. 2017. Classification of the printability of selected food for 3D printing: Development of an assessment method using hydrocolloids as reference material. *Journal of Food Engineering* 215:23–32. doi: 10.1016/j.jfoodeng.2017.07.017.

Kocaman, Y., T. U. Bulut, and O. Özcan. 2025. Mobile food printing in professional kitchens: An inquiry of potential use cases with novice chefs. *arXiv Preprint arXiv:2503.10116* 10.48550/arXiv.2503.10116.

Lee, C. P., M. J. Y. Ng, N. M. Y. Chian, and M. Hashimoto. 2024. Multi-material direct ink writing 3D food printing using multi-channel nozzle. *Future Foods* 10:100376–85. doi: 10.1016/j.fufo.2024.100376.

Lee, J. 2021. A 3D food printing process for the new normal era: A review. *Processes* 9 (9):1495–515. doi: 10.3390/pr9091495.

Lenie, M. D. R., S. Ahmadzadeh, F. V. Bockstaele, and A. Ubeyitogullari. 2024. Development of a pH-responsive system based on starch and alginate-pectin hydrogels using coaxial 3D food printing. *Food Hydrocolloids*. 153:109989–10000. doi: 10.1016/j.foodhyd.2024.109989.

Li, G., B. Wang, W. Lv, L. Yang, and H. Xiao. 2024. Effect of κ-carrageenan on physicochemical and 3D printing properties of walnut protein-stabilized emulsion gel. *Food Hydrocolloids*. 156:110288–99. doi: 10.1016/j.foodhyd.2024.110288.

Li, X., L. Fan, R. Li, Y. Han, and J. Li. 2023. 3D/4d printing of β-cyclodextrin-based high internal phase emulsions. *Journal of Food Engineering* 348:111455–65. doi: 10.1016/j.jfoodeng.2023.111455.

Li, X., L. Fan, Y. Liu, and J. Li. 2023. New insights into food O/W emulsion gels: Strategies of reinforcing mechanical properties and outlook of being applied to food 3D printing. *Critical Reviews in Food Science and Nutrition* 63 (11):1564–86. doi: 10.1080/10408398.2021.1965953.

Li, X., W. Liu, Z. Hu, C. He, J. Ding, W. Chen, S. Wang, and W. Dong. 2024. Supportless 3D-printing of non-planar thin-walled structures with the multi-axis screw-extrusion additive manufacturing system. *Materials & Design* 240:112860–9. doi: 10.1016/j.matdes.2024.112860.

Li, X., Y. Han, Y. Chen, W. Liu, L. Li, J. Chen, G. Ren, X. Li, Z. Luo, L. Pan, et al. 2025. Effects of chlorogenic acid on the physicochemical properties, 3D printing characteristics, and anti-digestive properties of sweet potato starch. *International Journal of Biological Macromolecules* 288:138726–37. doi: 10.1016/j.ijbiomac.2024.138726.

Li, Y., N. Xiang, Y. Zhu, M. Yang, C. Shi, Y. Tang, W. Sun, K. Sheng, D. Liu, and X. Zhang. 2024. Blue source-based food alternative

proteins: Exploring aquatic plant-based and cell-based sources for sustainable nutrition. *Trends in Food Science & Technology* 147:104439–52. doi: 10.1016/j.tifs.2024.104439.

Li, Z., S. Wang, Z. Qin, W. Fang, Z. Guo, and X. Zou. 2024. 3D printing properties of heat-induced sodium alginate–whey protein isolate edible gel. *Gels (Basel, Switzerland)* 10 (7):425–39. doi: 10.3390/gels10070425.

Lin, D., A. L. Kelly, and S. Miao. 2020. Preparation, structure-property relationships and applications of different emulsion gels: Bulk emulsion gels, emulsion gel particles, and fluid emulsion gels. *Trends in Food Science & Technology* 102:123–37. doi: 10.1016/j.tifs.2020.05.024.

Lin, J., C. Liang, T. Lin, R. Zhong, Y. Cao, and Y. Lan. 2025. Optimizing 3D food printing inks: The impact of polysaccharides on Camellia seed protein emulsion gels. *Food Hydrocolloids*. 166:111337–48. doi: 10.1016/j.foodhyd.2025.111337.

Liu, B., Y. Zhao, Y. Li, L. Tao, P. Pan, Y. Bi, S. Song, and L. Yu. 2024. Investigation of the structure, rheology and 3D printing characteristics of corn starch regulated by glycyrrhizic acid. *International Journal of Biological Macromolecules* 263 (Pt 1):130277–86. doi: 10.1016/j.ijbiomac.2024.130277.

Liu, L., T. Xie, W. Cheng, Y. Ding, and B. Xu. 2024. Characterization and mechanism of thermally induced tea polyphenols and egg white proteins gel system and its 3D printing. *Lwt* 205:116488–97. doi: 10.1016/j.lwt.2024.116488.

Liu, L., Y. Meng, X. Dai, K. Chen, and Y. Zhu. 2019. 3D printing complex egg white protein objects: Properties and optimization. *Food and Bioprocess Technology* 12 (2):267–79. doi: 10.1007/s11947-018-2209-z.

Liu, W., H. Hu, D. J. McClements, Z. Jin, and L. Chen. 2025. Fabrication and characterization of edible inks for 3D printing of dysphagia foods based on corn starch stabilized by calcium ions and hydrocolloids. *Food Hydrocolloids*. 166:111278–89. doi: 10.1016/j.foodhyd.2025.111278.

Liu, X., Y. Cheng, T. Sun, Y. Lu, S. Huan, S. Liu, W. Li, Z. Li, Y. Liu, O. J. Rojas, et al. 2025. Recent advances in plant-based edible emulsion gels for 3D-printed foods. *Annual Review of Food Science and Technology* 16 (1):63–79. doi: 10.1146/annurev-food-111523-121736.

Liu, Y., W. Y. Yu, X. L. Yu, Q. Tong, S. W. Li, S. Prakash, and X. P. Dong. 2023. Hot melt extrusion with low-temperature deposition-coupling control improves the 3D printing accuracy of gelatin/fish pulp recombinant products. *Journal of Food Engineering* 349:111454–64. doi: 10.1016/j.jfoodeng.2023.111454.

Liu, Z., B. Bhandari, and M. Zhang. 2020. Incorporation of probiotics (Bifidobacterium animalis subsp. Lactis) into 3D printed mashed potatoes: Effects of variables on the viability. *Food Research International (Ottawa, Ont.)* 128:108795–805. doi: 10.1016/j.foodres.2019.108795.

Llamas-Unzueta, R., A. Reguera-García, M. A. Montes-Morán, and J. A. Menéndez. 2025. Porous carbons with complex 3D geometries via selective laser sintering of whey powder. *Scientific Reports* 15 (1):1881–91. doi: 10.1038/s41598-024-84976-y.

Lu, S., S. Diao, X. Hu, Q. Wu, C. Bai, B. Xu, T. Ma, and Y. Song. 2025. Enhancement effect of cellulose nanocrystal on the rheological properties and 3D printing performance of pea protein isolate-based hydrogels. *Food Hydrocolloids*. 168:111477–87. doi: 10.1016/j.foodhyd.2025.111477.

Lupton, D., and B. Turner. 2018. Food of the future? Consumer responses to the idea of 3D-printed meat and insect-based foods. *Food and Foodways* 26 (4):269–89. doi: 10.1080/07409710.2018.1531213.

Lv, Y., W. Lv, G. Li, and Y. Zhong. 2023. The research progress of physical regulation techniques in 3D food printing. *Trends in Food Science & Technology* 133:231–43. doi: 10.1016/j.tifs.2023.02.004.

M'Barki, A., L. Bocquet, and A. Stevenson. 2017. Linking rheology and printability for dense and strong ceramics by direct ink writing. *Scientific Reports* 7 (1):6017–26. doi: 10.1038/s41598-017-06115-0.

Ma, T., R. Cui, S. Lu, X. Hu, B. Xu, Y. Song, and X. Hu. 2022. High internal phase Pickering emulsions stabilized by cellulose nanocrystals for 3D printing. *Food Hydrocolloids*. 125:107418–27. doi: 10.1016/j.foodhyd.2021.107418.

Ma, Y., and L. Zhang. 2022. Formulated food inks for extrusion-based 3D printing of personalized foods: A mini review. *Current Opinion in Food Science* 44:100803–8. doi: 10.1016/j.cofs.2021.12.012.

Ma, Y., J. Potappel, A. Chauhan, M. A. I. Schutyser, R. M. Boom, and L. Zhang. 2023. Improving 3D food printing performance using computer vision and feedforward nozzle motion control. *Journal of Food Engineering* 339:111277–89. doi: 10.1016/j.jfoodeng.2022.111277.

Miao, W., Y. Fu, Z. Zhang, Q. Lin, X. Li, S. Sang, D. J. McClements, H. Jiang, H. Ji, C. Qiu, et al. 2024. Fabrication of starch-based oleogels using capillary bridges: Potential for application as edible inks in 3D food printing. *Food Hydrocolloids*. 150:109647–56. doi: 10.1016/j.foodhyd.2023.109647.

Mobaraki, M., M. Ghaffari, A. Yazdanpanah, Y. Luo, and D. K. Mills. 2020. Bioinks and bioprinting: A focused review. *Bioprinting* 18:e00080-95. doi: 10.1016/j.bprint.2020.e00080.

Montoya, J., J. Medina, A. Molina, J. Gutiérrez, B. Rodríguez, and R. Marín. 2021. Impact of viscoelastic and structural properties from starch-mango and starch-arabinoxylans hydrocolloids in 3D food printing. *Additive Manufacturing* 39:101891–9. doi: 10.1016/j.addma.2021.101891.

Mu, R. Y., B. Wang, W. Q. Lv, J. Yu, and G. H. Li. 2023. Improvement of extrudability and self-support of emulsion-filled starch gel for 3D printing: Increasing oil content. *Carbohydrate Polymers* 301 (Pt A):120293–303. doi: 10.1016/j.carbpol.2022.120293.

Nam, H. K., T. W. Kang, I. Kim, R. Choi, H. W. Kim, and H. J. Park. 2023. Physicochemical properties of cricket (Gryllus bimaculatus) gel fraction with soy protein isolate for 3D printing-based meat analogue. *Food Bioscience* 53:102772–81. doi: 10.1016/j.fbio.2023.102772.

Navaf, M., K. V. Sunooj, B. Aaliya, P. P. Akhila, C. Sudheesh, S. A. Mir, and J. George. 2022. 4D printing: A new approach for food printing; effect of various stimuli on 4D printed food properties. A comprehensive review. *Applied Food Research* 2 (2):100150–61. doi: 10.1016/j.afres.2022.100150.

Noree, S., Y. Pinyakit, N. Tungkijanansin, C. Kulsing, and V. P. Hoven. 2023. Shape transformation of 4D printed edible insects triggered by thermal dehydration. *Journal of Food Engineering* 358:111666–73. doi: 10.1016/j.jfoodeng.2023.111666.

Oh, Y., S. Lee, N. K. Lee, and J. Rhee. 2024. Improving the three-dimensional printability of potato starch loaded onto food ink. *Journal of Microbiology and Biotechnology* 34 (4):891–901. doi: 10.4014/jmb.2311.11040.

Oliveira, S. M., A. J. Martins, P. Fuciños, M. A. Cerqueira, and L. M. Pastrana. 2023. Food additive manufacturing with lipid-based inks: Evaluation of phytosterol-lecithin oleogels. *Journal of Food Engineering* 341:111317–26. doi: 10.1016/j.jfoodeng.2022.111317.

Oyinloye, T. M., and W. B. Yoon. 2021. Stability of 3D printing using a mixture of pea protein and alginate: Precision and application of additive layer manufacturing simulation approach for stress distribution. *Journal of Food Engineering* 288:110127–39. doi: 10.1016/j.jfoodeng.2020.110127.

Palla, C. A., M. Dominguez, and M. E. Carrín. 2022. An overview of structure engineering to tailor the functionality of monoglyceride oleogels. *Comprehensive Reviews in Food Science and Food Safety* 21 (3):2587–614. doi: 10.1111/1541-4337.12930.

Perța-Crișan, S., C. Ursachi, B. Chereji, I. Tolan, and F. Munteanu. 2023. Food-grade oleogels: Trends in analysis, characterization, and applicability. *Gels (Basel, Switzerland)* 9 (5):386–427. doi: 10.3390/gels9050386.

Phuhongsung, P., M. Zhang, and S. Devahastin. 2020. Influence of surface pH on color, texture and flavor of 3D printed composite mixture of soy protein isolate, pumpkin, and beetroot. *Food and Bioprocess Technology* 13 (9):1600–10. doi: 10.1007/s11947-020-02497-8.

Pinto, T. C., A. J. Martins, L. Pastrana, M. C. Pereira, and M. A. Cerqueira. 2021. Oleogel-based systems for the delivery of bioactive compounds in foods. *Gels (Basel, Switzerland)* 7 (3):86–109. doi: 10.3390/gels7030086.

Qian, S., X. Jiang, P. F. Qian, B. Zi, and W. D. Zhu. 2024. Calibration of static errors and compensation of dynamic errors for cable-driven parallel 3D printer. *Journal of Intelligent & Robotic Systems* 110 (1):1–18. doi: 10.1007/s10846-024-02062-x.

Ratnayake, W. S., and D. S. Jackson. 2009. Starch gelatinization. *Advances in Food and Nutrition Research* 55:221–68. doi: 10.1016/S1043-4526(08)00405-1.

Saleem, W., D. Chimene, B. P. White, K. A. Deo, J. L. Thomas, N. Chidambara, C. Mandrona, K. Landsgaard, B. Ko, R. Kaunas, et al. 2025. IN4MER bioink: A phosphorescent biosensing bio-ink for multiple analytes (glucose, lactate, oxygen) measurements and temperature sensing applications. *bioRxiv* 2025-04. doi: 10.1101/2025.04.22.650078.

Samandari, M., F. Saeedinejad, J. Quint, S. X. Y. Chuah, R. Farzad, and A. Tamayol. 2023. Repurposing biomedical muscle tissue engineering for cellular agriculture: Challenges and opportunities. *Trends in Biotechnology* 41 (7):887–906. doi: 10.1016/j.tibtech.2023.02.002.

Shah, P. L. 1997. Melt rheology and its role in plastics processing, 97–8. Wiley Online Library. doi: 10.1002/vnl.10172.

Shahrubudin, N., T. C. Lee, and R. Ramlan. 2019. An overview on 3D printing technology: Technological, materials, and applications. *Procedia Manufacturing* 35:1286–96. doi: 10.1016/j.promfg.2019.06.089.

Sharma, R., P. C. Nath, T. K. Hazarika, A. Ojha, P. K. Nayak, and K. Sridhar. 2024. Recent advances in 3D printing properties of natural food gels: Application of innovative food additives. *Food Chemistry* 432:137196–206. doi: 10.1016/j.foodchem.2023.137196.

Shi, H., M. Zhang, and A. S. Mujumdar. 2024. 3D/4D printed super reconstructed foods: Characteristics, research progress, and prospects. *Comprehensive Reviews in Food Science and Food Safety* 23 (2):e13310-41. doi: 10.1111/1541-4337.13310.

Shi, Y., M. Zhang, and P. Phuhongsung. 2022. Microwave-induced spontaneous deformation of purple potato puree and oleogel in 4D printing. *Journal of Food Engineering* 313:110757–66. doi: 10.1016/j.jfoodeng.2021.110757.

Singh, M., P. Sharma, S. K. Sharma, and J. Singh. 2025. A novel real-time quality control system for 3D printing: A deep learning approach using data efficient image transformers. *Expert Systems with Applications* 273 (10):126863–80. doi: 10.1016/j.eswa.2025.126863.

Sonaye, S. Y., E. G. Ertugral, C. R. Kothapalli, and P. Sikder. 2022. Extrusion 3D (bio) printing of alginate-gelatin-based composite scaffolds for skeletal muscle tissue engineering. *Materials (Basel, Switzerland)* 15 (22):7945–68. doi: 10.3390/ma15227945.

Song, J., J. Huang, S. Ren, H. Zheng, D. Zhou, and L. Song. 2024. Cultivating edible bio-inks: Elevating 3D printing with medium-internal-phase emulsion gel incorporating soybean protein isolate microgel particles. *Food Hydrocolloids.* 149:109582–94. doi: 10.1016/j.foodhyd.2023.109582.

Song, K., B. Ren, Y. Zhai, W. Chai, and Y. Huang. 2021. Effects of transglutaminase cross-linking process on printability of gelatin microgel-gelatin solution composite bioink. *Biofabrication* 14 (1):015014–28. doi: 10.1088/1758-5090/ac3d75.

Su, C., Y. Wu, B. Vardhanabhuti, and M. Lin. 2025. 4D printing of dysphagia foods using pea protein and purple sweet potato flour. *Food Bioscience* 64:105887–95. doi: 10.1016/j.fbio.2025.105887.

Sui, X., T. Zhang, and L. Jiang. 2021. Soy protein: Molecular structure revisited and recent advances in processing technologies. *Annual Review of Food Science and Technology* 12 (1):119–47. doi: 10.1146/annurev-food-062220-104405.

Sun, J., W. Zhou, L. Yan, D. Huang, and L. Lin. 2018. Extrusion-based food printing for digitalized food design and nutrition control. *Journal of Food Engineering* 220:1–11. doi: 10.1016/j.jfoodeng.2017.02.028.

Tamir, T. S., G. Xiong, Q. Fang, Y. Yang, Z. Shen, M. Zhou, and J. Jiang. 2023. Machine-learning-based monitoring and optimization of processing parameters in 3D printing. *International Journal of Computer Integrated Manufacturing* 36 (9):1362–78. doi: 10.1080/0951192X.2022.2145019.

Tamir, T. S., G. Xiong, Q. H. Fang, X. S. Dong, Z. Shen, and F. Y. Wang. 2022. A feedback-based print quality improving strategy for FDM 3D printing: An optimal design approach. *The International Journal of Advanced Manufacturing Technology* 120 (3-4):2777–91. doi: 10.1007/s00170-021-08332-4.

Tan, J. J. Y., C. P. Lee, and M. Hashimoto. 2020. Preheating of gelatin improves its printability with transglutaminase in direct ink writing 3D printing. *International Journal of Bioprinting* 6 (4):296–307. doi: 10.18063/ijb.v6i4.296.

Teng, X., M. Zhang, and A. S. Mujumdar. 2021. 4D printing: Recent advances and proposals in the food sector. *Trends in Food Science & Technology* 110:349–63. doi: 10.1016/j.tifs.2021.01.076.

Tezel, T., and V. Kovan. 2022. Determination of optimum production parameters for 3D printers based on nozzle diameter. *Rapid Prototyping Journal* 28 (1):185–94. doi: 10.1108/RPJ-08-2020-0185.

Tian, H., J. Wu, Y. Hu, X. Chen, X. Cai, Y. Wen, H. Chen, J. Huang, and S. Wang. 2024. Recent advances on enhancing 3D printing quality of protein-based inks: A review. *Comprehensive Reviews in Food Science and Food Safety* 23 (3):e13349-71. doi: 10.1111/1541-4337.13349.

Tian, Z., Q. Zhong, H. Zhang, T. Yin, J. Zhao, G. Liu, Y. Zhao, H. N. Li, and Y. He. 2024. Optimising printing fidelity of the single-nozzle based multimaterial direct ink writing for 3D food printing. *Virtual and Physical Prototyping* 19 (1):e2352075-85. doi: 10.1080/17452759.2024.2352075.

Tong, Q., Y. Jiang, S. Xiao, Y. Meng, and X. Dong. 2024. Research on improving the structural stability of surimi 3D printing through laser cooking techniques. *Journal of Food Engineering* 375:112075–87. doi: 10.1016/j.jfoodeng.2024.112075.

Tran, P. H. L., B. Lee, and T. T. D. Tran. 2021. Recent studies on the processes and formulation impacts in the development of solid dispersions by hot-melt extrusion. *European Journal of Pharmaceutics and Biopharmaceutics: Official Journal of Arbeitsgemeinschaft Fur Pharmazeutische Verfahrenstechnik e.V* 164:13–9. doi: 10.1016/j.ejpb.2021.04.009.

Ulagesan, S., S. Krishnan, T. Nam, and Y. Choi. 2024. Production of fish fillet analogues using novel fish muscle cell powder and sodium alginate-κ-carrageenan based bio-ink. *Food Hydrocolloids.* 157:110446–60. doi: 10.1016/j.foodhyd.2024.110446.

Vadodaria, S., and T. Mills. 2020. Jetting-based 3D printing of edible materials. *Food Hydrocolloids.* 106:105857–60. doi: 10.1016/j.foodhyd.2020.105857.

Varvara, R., K. Szabo, and D. C. Vodnar. 2021. 3D food printing: Principles of obtaining digitally-designed nourishment. *Nutrients* 13 (10):3617–37. doi: 10.3390/nu13103617.

Wang, J., Q. Jiang, Z. Huang, A. H. Muhammad, A. Gharsallaoui, M. Cai, K. Yang, and P. Sun. 2024. Rheological and mechanical behavior of soy protein-polysaccharide composite paste for extrusion-based 3D food printing: Effects of type and concentration of polysaccharides. *Food Hydrocolloids.* 153:109942–52. doi: 10.1016/j.foodhyd.2024.109942.

Wang, J., X. Jiang, H. Gan, S. Li, K. Peng, Y. Sun, M. Ma, and Y. Yi. 2025. Complexation-driven 3D printable whey protein-lotus root composite gels for dysphagia foods. *Carbohydrate Polymers* 366 (15):123864–77. doi: 10.1016/j.carbpol.2025.123864.

Wang, N., R. Li, X. Wang, and X. Yang. 2024. 4D food printing: Key factors and optimization strategies. *Trends in Food Science & Technology* 145:104380–91. doi: 10.1016/j.tifs.2024.104380.

Wang, S., Y. Zhang, L. Chen, X. Xu, G. Zhou, Z. Li, and X. Feng. 2018. Dose-dependent effects of rosmarinic acid on formation of oxidatively stressed myofibrillar protein emulsion gel at different NaCl concentrations. *Food Chemistry* 243:50–7. doi: 10.1016/j.foodchem.2017.09.114.

Wang, T., S. Lu, X. Hu, B. Xu, C. Bai, T. Ma, and Y. Song. 2024. Cellulose nanocrystals-gelatin composite hydrocolloids: Application to controllable responsive deformation during 3D printing. *Food Hydrocolloids.* 151:109780–9. doi: 10.1016/j.foodhyd.2024.109780.

Wang, Y., D. J. McClements, C. Bai, X. Xu, Q. Sun, B. Jiao, S. Miao, Q. Wang, and L. Dai. 2024. Application of proteins in edible inks for 3D food printing: A review. *Trends in Food Science & Technology* 153:104691–701. doi: 10.1016/j.tifs.2024.104691.

Wang, Y., Q. Liu, Y. Yang, R. Zhang, A. Jiao, and Z. Jin. 2023. Construction of transglutaminase covalently cross-linked hydrogel and high internal phase emulsion gel from pea protein modified by high-intensity ultrasound. *Journal of the Science of Food and Agriculture* 103 (4):1874–84. doi: 10.1002/jsfa.12372.

Wang, Y., R. E. Aluko, D. J. McClements, Y. Yu, X. Xu, Q. Sun, Q. Wang, B. Jiao, and L. Dai. 2024. Emulsion gel-based inks for 3D printing of foods for dysphagia patients: High internal type emulsion gel-biopolymer systems. *Food Hydrocolloids.* 156:110340–54. doi: 10.1016/j.foodhyd.2024.110340.

Wedamulla, N. E., Y. Choi, Q. Zhang, S. Kim, H. Kang, and E. Kim. 2024. Citrus peel powder alters the rheological properties and 3D printing performance of potato starch gel. *International Journal of*

Biological Macromolecules 279 (Pt 1):135229–45. doi: 10.1016/j.ijbiomac.2024.135229.

Wen, Y., C. Chao, Q. T. Che, H. W. Kim, and H. J. Park. 2023. Development of plant-based meat analogs using 3D printing: Status and opportunities. *Trends in Food Science & Technology* 132:76–92. doi: 10.1016/j.tifs.2022.12.010.

Wu, J., H. Zhu, and C. Li. 2024. Potential sources of novel proteins suitable for use as ingredients in 3D food printing, along with some of the food safety challenges. *International Journal of Gastronomy and Food Science* 37:100983–93. doi: 10.1016/j.ijgfs.2024.100983.

Xia, G., L. Tao, S. Zhang, X. Hao, and S. Ou. 2024. An optimization study of 3D Printing technology utilizing a hybrid gel system based on astragalus polysaccharide and wheat starch. *Processes* 12 (9):1898. doi: 10.3390/pr12091898.

Xiao, K., J. Zhang, L. Pan, and K. Tu. 2024. Investigation of 3D printing product of powder-based white mushroom incorporated with soybean protein isolate as dysphagia diet. *Food Research International (Ottawa, Ont.)* 175:113760–76. doi: 10.1016/j.foodres.2023.113760.

Xiao, S., J. Yang, Y. Bi, Y. Li, Y. Cao, M. Zhou, G. Pang, X. Dong, and Q. Tong. 2025. Food 3D printing equipment and innovation: Precision meets edibility. *Foods (Basel, Switzerland)* 14 (12):2066–76. doi: 10.3390/foods14122066.

Xie, J., J. Bi, X. Liu, C. Blecker, N. Jacquet, and J. Lyu. 2025. Development of soy protein isolate-chelator soluble pectin composite gels as extrusion-based 3D food printing inks: Effects of mingling strategy. *Food Hydrocolloids.* 162:110904–14. doi: 10.1016/j.foodhyd.2024.110904.

Xu, B., X. Wang, B. Chitrakar, Y. Xu, B. Wei, B. Wang, L. Lin, Z. Guo, C. Zhou, and H. Ma. 2025. Effect of various physical modifications of pea protein isolate (PPI) on 3D printing behavior and dysphagia properties of strawberry-PPI gels. *Food Hydrocolloids.* 158:110498–508. doi: 10.1016/j.foodhyd.2024.110498.

Yoha, K. S., T. Anukiruthika, W. Anila, J. A. Moses, and C. Anandharamakrishnan. 2021. 3D printing of encapsulated probiotics: Effect of different post-processing methods on the stability of Lactiplantibacillus plantarum (NCIM 2083) under static in vitro digestion conditions and during storage. *Lwt* 146:111461–9. doi: 10.1016/j.lwt.2021.111461.

Yu, J., R. Qiu, W. Zheng, K. Wang, X. Liu, Z. Hu, and L. Zhao. 2025. Multiphase gel-based functional inks in 3D food printing: A review on structural design and enhanced bioaccessibility of active ingredients. *Food Research International (Ottawa, Ont.)* 217:116787–98. doi: 10.1016/j.foodres.2025.116787.

Zampouni, K., A. Soniadis, T. Moschakis, C. G. Biliaderis, A. Lazaridou, and E. Katsanidis. 2022. Crystalline microstructure and physicochemical properties of olive oil oleogels formulated with monoglycerides and phytosterols. *Lwt* 154:112815–24. doi: 10.1016/j.lwt.2021.112815.

Zeng, X., T. Li, J. Zhu, L. Chen, and B. Zheng. 2021. Printability improvement of rice starch gel via catechin and procyanidin in hot extrusion 3D printing. *Food Hydrocolloids.* 121:106997–7005. doi: 10.1016/j.foodhyd.2021.106997.

Zhang, C., C. Wang, M. Girard, D. Therriault, and M. Heuzey. 2024. 3D printed protein/polysaccharide food simulant for dysphagia diet: Impact of cellulose nanocrystals. *Food Hydrocolloids.* 148:109455–69. doi: 10.1016/j.foodhyd.2023.109455.

Zhang, H., S. Hua, M. Liu, R. Chuang, X. Gao, H. Li, N. Xia, and C. Xiao. 2025. Citric acid improves egg white protein foaming characteristics and meringue 3D printing performance. *Foods (Basel, Switzerland)* 14 (2):198–218. doi: 10.3390/foods14020198.

Zhang, L., A. A. Zaky, C. Zhou, Y. Chen, W. Su, H. Wang, A. M. A. El-Aty, and M. Tan. 2022. High internal phase Pickering emulsion stabilized by sea bass protein microgel particles: Food 3D printing application. *Food Hydrocolloids.* 131:107744–56. doi: 10.1016/j.foodhyd.2022.107744.

Zhao, W., Z. Wei, and C. Xue. 2022. Recent advances on food-grade oleogels: Fabrication, application and research trends. *Critical Reviews in Food Science and Nutrition* 62 (27):7659–76. doi: 10.1080/10408398.2021.1922354.

Zheng, L., A. Ren, R. Liu, Y. Xing, X. Yu, and H. Jiang. 2022. Effect of sodium chloride solution on quality of 3D-printed samples molded using wheat starch gel. *Food Hydrocolloids.* 123:107197–206. doi: 10.1016/j.foodhyd.2021.107197.

Zheng, L., J. Liu, R. Liu, Y. Xing, and H. Jiang. 2021. 3D printing performance of gels from wheat starch, flour and whole meal. *Food Chemistry* 356:129546–54. doi: 10.1016/j.foodchem.2021.129546.

Zhong, Y., B. Wang, W. Lv, Y. Wu, Y. Lv, and S. Sheng. 2024. Recent research and applications in lipid-based food and lipid-incorporated bioink for 3D printing. *Food Chemistry* 458 (15):140294–306. doi: 10.1016/j.foodchem.2024.140294.

Zhou, J., H. Li, L. Lu, and Y. Cheng. 2024. Machine vision-based surface defect detection study for ceramic 3D printing. *Machines* 12 (3):166–80. doi: 10.3390/machines12030166.

Zhu, J. C., Y. Cheng, Z. Y. Ouyang, Y. X. Yang, L. Ma, H. X. Wang, and Y. H. Zhang. 2023. 3D printing surimi enhanced by surface crosslinking based on dry-spraying transglutaminase, and its application in dysphagia diets. *Food Hydrocolloids.* 140:108600–10. doi: 10.1016/j.foodhyd.2023.108600.

Zhu, S. C., M. Ribberink, M. de Wit, M. Schutyser, and M. Stieger. 2020. Modifying sensory perception of chocolate coated rice waffles through bite-to-bite contrast: An application case study using 3D inkjet printing. *Food & Function* 11 (12):10580–7. doi: 10.1039/d0fo01787f.

Zhu, S., P. V. Ramos, O. R. Heckert, M. Stieger, A. J. van der Goot, and M. Schutyser. 2022. Creating protein-rich snack foods using binder jet 3D printing. *Journal of Food Engineering* 332:111124–34. doi: 10.1016/j.jfoodeng.2022.111124.